https://doi.org/10.1093/plcell/koad192 THE PLANT CELL 2023: 35: 3889–3910

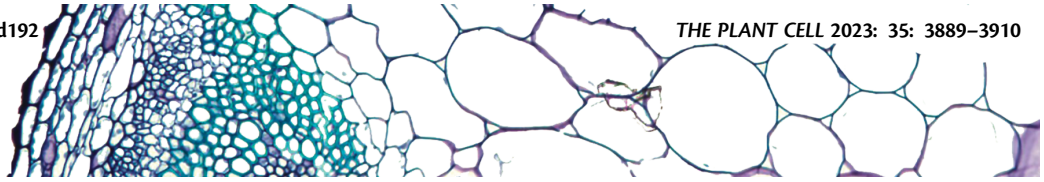

Research Article

Thermosensitive SUMOylation of TaHsfA1 defines a dynamic ON/OFF molecular switch for the heat stress response in wheat

Haoran Wang [1,†] Man Feng [1,2,†] Yujie Jiang [1,†] Dejie Du [1] Chaoqun Dong [1] Zhaoheng Zhang [1] Wenxi Wang [1] Jing Liu [1] Xiangqing Liu [1] Sufang Li [1] Yongming Chen [1] Weilong Guo [1] Mingming Xin [1] Yingyin Yao [1] Zhongfu Ni [1] Qixin Sun [1] Huiru Peng [1] and Jie Liu [1,*]

1 Frontiers Science Center for Molecular Design Breeding, Key Laboratory of Crop Heterosis and Utilization (MOE), Beijing Key Laboratory of Crop Genetic Improvement, College of Agronomy and Biotechnology, China Agricultural University, Beijing 100193, China
2 National Key Laboratory of Crop Genetic Improvement and National Center of Plant Gene Research, College of Plant Science and Technology, Huazhong Agricultural University, Wuhan 430070, China

*Author for correspondence: jieliu@cau.edu.cn
†These authors contributed equally.

Abstract

Dissecting genetic components in crop plants associated with heat stress (HS) sensing and adaptation will facilitate the design of modern crop varieties with improved thermotolerance. However, the molecular mechanisms underlying the ON/OFF switch controlling HS responses (HSRs) in wheat (*Triticum aestivum*) remain largely unknown. In this study, we focused on the molecular action of TaHsfA1, a class A heat shock transcription factor, in sensing dynamically changing HS signals and regulating HSRs. We show that the TaHsfA1 protein is modified by small ubiquitin–related modifier (SUMO) and that this modification is essential for the full transcriptional activation activity of TaHsfA1 in triggering downstream gene expression. During sustained heat exposure, the SUMOylation of TaHsfA1 is suppressed, which partially reduces TaHsfA1 protein activity, thereby reducing the intensity of downstream HSRs. In addition, we demonstrate that TaHsfA1 interacts with the histone acetyltransferase TaHAG1 in a thermosensitive manner. Together, our findings emphasize the importance of TaHsfA1 in thermotolerance in wheat. In addition, they define a highly dynamic SUMOylation-dependent "ON/OFF" molecular switch that senses temperature signals and contributes to thermotolerance in crops.

Introduction

Global warming in recent decades has had adverse effects on crop production. In particular, prolonged periods of higher-than-optimum temperatures heavily suppress carbon assimilation and starch synthesis, which leads to decreased grain yields (Li et al. 2018). It was estimated that for every 1 °C increase in the mean global temperature, bread wheat (*Triticum aestivum*) yield will decrease by ∼6%, and rice (*Oryza sativa*) yield will decrease by 3.2% (Zhao et al. 2017; Li et al. 2018). Therefore, it is urgent to dissect the genetic networks associated with heat stress (HS) sensing and adaptation in crops, which will facilitate the design of crop varieties with improved thermotolerance via molecular breeding.

Heat shock transcription factors (Hsfs) are a class of DNA-binding proteins that play central roles in promoting rapid heat-induced transcriptional reprogramming. Upon the perception of HS, Hsfs recognize highly conserved heat shock elements (HSEs, 5′-nGAAnnTTCn-3′) in the promoters of large groups of heat-inducible heat shock protein (*HSP*)

Received October 27, 2022. Accepted June 12, 2023. Advance access publication July 3, 2023

IN A NUTSHELL

Background: In response to high temperature, plants use transcription factors to initiate protective responses; as they acclimate to extended high temperature, the plants then turn off these rapid responses. The heat shock–associated transcription factor HsfA1 plays a central role in sensing heat stress and promoting rapid transcriptional responses. At normal temperatures, HsfA1 is associated with heat shock proteins such as HSP70 and HSP90, which repress its protein activity; at high temperature, these proteins rapidly release HsfA1 to initiate heat stress responses. In addition to this well-known OFF-to-ON switch for HsfA1 activity, additional ON-to-OFF mechanisms must exist to complete the HsfA1 cycle during acclimation to long-term heat stress. Here we explored how the ON/OFF molecular regulation of HsfA1 activity occurs in wheat (*Triticum aestivum*).

Question: How is the transcriptional activation activity of HsfA1 regulated when it is released from multichaperone repression complexes during prolonged periods of high temperatures?

Findings: Genetic evidence revealed that TaHsfA1 is required for basal and acquired thermotolerance as well as normal heat-induced transcriptional reprogramming in wheat. TaHsfA1 is modified by the small peptide small ubiquitin–related modifier predominantly at its 459th amino acid (lysine, K459). SUMOylated TaHsfA1 proteins were detected at the early stage of heat stress treatment, but their levels decreased upon prolonged thermal stress. Consistent with these observations, heat stress–responsive genes were highly induced at the beginning of heat shock but were downregulated and returned to basal expression levels during long-term thermal stress. These findings support a role for the thermosensitive SUMOylation of TaHsfA1 in controlling TaHsfA1 activity and dynamic heat stress responses at different stages of thermal stress.

Next steps: We plan to introduce the K459-mutated (non-SUMOylated) form of TaHsfA1 into wheat *Tahsfa1* mutants to evaluate the importance of TaHsfA1 SUMOylation in sensing heat stress and regulating responses in cereal crops. In addition, we plan to look for the protein components responsible for TaHsfA1 deSUMOylation during long-term thermal stress.

genes (encoding protective chaperones) to transiently activate HS responses (HSRs) (Andrási et al. 2021). This Hsf-triggered signal transduction occurs very quickly, normally within 5 min (Liu et al. 2003; Li et al. 2019).

Plants possess multiple Hsf isoforms. For example, the model plant *Arabidopsis thaliana* (Arabidopsis) contains 21 Hsfs, rice contains 25 Hsfs, and tomato (*Solanum lycopersicum*) contains 24 Hsfs (Nover et al. 2001; Scharf et al. 2012). However, the specific roles of these Hsfs have only been extensively described in a few plant species. In Arabidopsis, for example, the 21 Hsfs were assigned to 3 different classes, with 15 members belonging to class A (HsfA1 to HsfA9), 5 members belonging to class B (HsfB1 to HsfB4), and 1 member belonging to class C. Among these, the A class Hsf members are considered to be the most important transcriptional activators responsible for the initiation of HSRs, while HsfBs are likely transcriptional repressors. Although the genetic and physical interactions among different classes of Hsfs are extremely complicated and still largely elusive, it is widely accepted that HsfA1s function as hubs of HS-responsive transcriptional cascades in plants (Mishra et al. 2002; Scharf et al. 2012; Andrási et al. 2021). Indeed, more than 65% of HS-induced genes, including the transcription factor genes *HsfA2*, *HsfB1*, *MULTIPROTEIN BRIDGING FACTOR1c* (*MBF1c*), and *DEHYDRATION-RESPONSIVE ELEMENT-BINDING PROTEIN 1A* (*DREB1A*), which contribute to thermotolerance, cannot be upregulated during HS after the loss of function of HsfA1 (Liu et al. 2011).

Due to the central role of HsfA1 in HSRs and thermotolerance, many studies have been carried out to dissect the molecular mechanisms underlying the modulation of HsfA1 activity. In mammals, Hsf1 exists in the cytoplasm, and its protein activity is blocked when it is associated with various HSPs, including HSP70, HSP90, and Hsf-binding protein 1 (HSBP1); upon heat shock recognition, Hsf1 is rapidly released from these Hsf1–HSP70/90/HSBP1 protein complexes, allowing the trimerization of Hsf1 and consequently the transcriptional activation of downstream HS-responsive genes (Satyal et al. 1998; Shi et al. 1998; Zou et al. 1998). Notably, the posttranslational regulation of Hsf1, including acetylation, phosphorylation, and SUMOylation, also influences Hsf1 activity, either positively or negatively (Xu et al. 2012). In particular, the stress-inducible deacetylation of Hsf1 by the deacetylase and longevity factor SIRT1 promotes Hsf1 binding to HSEs for effective activation of the HSR, while acetylation of Hsf1 attenuates the DNA-binding activity of Hsf1, which guarantees the timely release of Hsf1 from its targeting promoters during prolonged thermal stress to prevent HS oversensitivity (Westerheide et al. 2009). This provides a plausible model in mammalian cells to explain the dynamic Hsf1 cycle from an active to inactive state.

Similar to those in mammals, plant HsfA1s are also associated with HSP70/HSP90 chaperones, and their activities in facilitating downstream gene expression are tightly regulated (Sugio et al. 2009; Hahn et al. 2011; Yoshida et al.

2011; Zhao et al. 2021). In addition to HSP70 and HSP90, in Arabidopsis, HSBP1 also interacts with HsfA1a and HsfA1b to attenuate their DNA-binding activities (Hsu et al. 2010). However, the mechanisms underlying HsfA1 sequestration during or after thermal stress in plants are still elusive.

SUMOylation, i.e. the conjugation of the small ubiquitin–related modifier (SUMO) to targeted proteins, is a reversible posttranslational modification that frequently occurs in eukaryotic cells, especially under stress conditions (Yoo et al. 2006; Augustine and Vierstra 2018). For instance, the heat-induced SUMO modification can be induced very quickly by a temperature upshift, illustrating the involvement of SUMO modification in sensing HS signals (Kurepa et al. 2003; Miller et al. 2013; Rytz et al. 2018). In general, SUMO isoforms (such as SUMO1 and SUMO2) are covalently attached to their substrate proteins at the lysine residue of Ψ-K-X-D/E (Ψ: hydrophobic residue; K: lysine residue; X: any amino acid; and D/E: aspartic acid or glutamic acid residue) consensus motifs via their C-terminus. This process requires the activities of 3 enzymes, the E1 activating enzyme, E2 conjugating enzyme, and E3 SUMO ligases, such as SAP and MIZ1 domain-containing ligase 1 (SIZ1) (Augustine and Vierstra 2018; Rytz et al. 2018; Liebelt et al. 2019a; Liebelt et al. 2019b). Conversely, SUMOylation is counteracted by SUMO-specific proteases, such as ULPs, ASP1, ESD4, and SENPs (Castro et al. 2018; Morrell and Sadanandom 2019; Liebelt et al. 2019b).

It has been well documented that in response to HS, groups of thermotolerance-regulating components are SUMOylated, including Hsf1 and Hsf2 in mammals, as well as HsfA2, HsfB2b, and DREB2A in plants (Goodson et al. 2001; Hietakangas et al. 2003; Cohen-Peer et al. 2010; Miller et al. 2010, 2013; Rytz et al. 2018; Liebelt et al. 2019a; Wang et al. 2020; Kmiecik et al. 2021). However, the biological significance of SUMOylation is likely highly divergent in different eukaryotes. For example, in mammals, SUMOylation facilitates the DNA-binding activity of Hsf1 and Hsf2 for the promotion of HSRs, while in plants, SUMO modification of HsfA2 blocks the transcriptional activity of this transcription factor, leading to the attenuation of HSRs (Goodson et al. 2001; Hietakangas et al. 2003; Cohen-Peer et al. 2010).

Bread wheat is a typical allohexaploid (AABBDD, 2n = 6x = 42) staple food crop, and therefore, its *Hsf* genes are expected to be more complex than those of diploid plant species. Indeed, a recent study identified groups of *Hsf* genes in the wheat genome (Duan et al. 2019). Among these, 3 *TaHsfA1* homologs, i.e. *TaHsfA1-1* (on chromosome 4A), *TaHsfA1-2* (on chromosome 5B), and *TaHsfA1-3* (on chromosome 5D), have been identified (in this study, we renamed them *TaHsfA1-A*, *TaHsfA1-B*, and *TaHsfA1-D* to clearly designate their locations on different subgenomes) (Duan et al. 2019). However, their roles in regulating HSRs are currently unclear. In this study, we focused on the role of TaHsfA1 in sensing HS and triggering basal thermotolerance in wheat. Our data support a critical role of thermosensitive SUMOylation at a lysine residue of TaHsfA1 in facilitating the transcriptional activation activity of this key transcription factor. More importantly, sustained HS triggers the downregulation of TaHsfA1 SUMOylation, leading to the attenuation of TaHsfA1 activity and contributing to the resilience of HSRs. These findings define a dynamic and reversible active-to-inactive cycle of TaHsfA1 in response to HS that fine-tunes HSR intensity and facilitates the establishment of thermal adaptation in wheat.

Results

Characterization of *HsfA1* genes in wheat

Using the well-defined HsfA1 protein sequences from the model plant Arabidopsis and the crop plant tomato as queries, we searched for HsfA1 homolog proteins in the wheat genome based on the Chinese Spring (CS) reference genome (IWGSC RefSeq V1.1) (International Wheat Genome Sequencing Consortium (IWGSC) 2018). In total, 3 proteins deduced from the homoeologous genes TraesCS4A02G322300 (previously named *TaHsfA1-1*), TraesCS5B02G556200 (previously named *TaHsfA1-2*), and TraesCS5D02G553300 (previously named *TaHsfA1-3*) with ~97% identity were identified as TaHsfA1 candidates (Fig. 1A) (Duan et al. 2019). In this study, we renamed these *TaHsfA1* homoeologous genes as *TaHsfA1-A*, *TaHsfA1-B*, and *TaHsfA1-D*, respectively.

Among these 3 HsfA1 proteins, 7 highly conserved functional motifs were annotated: DNA-binding domain (DBD), heptad repeat A (HR-A), HR-B, nuclear localization signal (NLS), nuclear export signal (NES), HR-C, and AHA (transcriptional activation). Similar to SlHsfA1 from tomato, the TaHsfA1 proteins contain all 7 functional motifs (Figs. 1A, S1, and S2). Notably, in Arabidopsis, HR-C was not found in AtHsfA1a or AtHsfA1b, while AHA was not annotated in AtHsfA1d (Figs. 1A, S1, and S2).

Phylogenetic analysis of HsfA1 proteins from different angiosperms clustered the tribe Triticeae HsfA1 proteins into the same branch, which included bread wheat, its diploid relatives *Triticum urartu* (the donor of the A subgenome of wheat) and *Aegilops tauschii* (the donor of the D subgenome of wheat), and barley (*Hordeum vulgare*) (Fig. 1B). In addition, the HsfA1 proteins from dicot and monocot species were divided into different clusters (Fig. 1B and Supplemental Data Set 1), suggesting that the dicot- and monocot-originated HsfA1 proteins might be functionally different.

Previous studies in Arabidopsis and tomato showed that HsfA1s confer transcriptional activation activity via their carboxyl-terminal (CT) regions, which harbor a functional AHA motif (Döring et al. 2000; Kotak et al. 2004). Accordingly, we divided the TaHsfA1 protein (for the subsequent experiments, we used TaHsfA1-D and refer to it as TaHsfA1 throughout) into 3 truncated versions: the amino-terminus (NT, 1-150 aa, including DBD), middle region (MD, 151-300 aa including the HR-A/B region and NLS), and CT (301-522 aa including the NES, HR-C, and AHA motifs) (Fig. 1C), to identify the domain responsible for the transcriptional activation activity of TaHsfA1. Fusion of these truncated versions (NT, MD, and CT) with GAL4-BD and

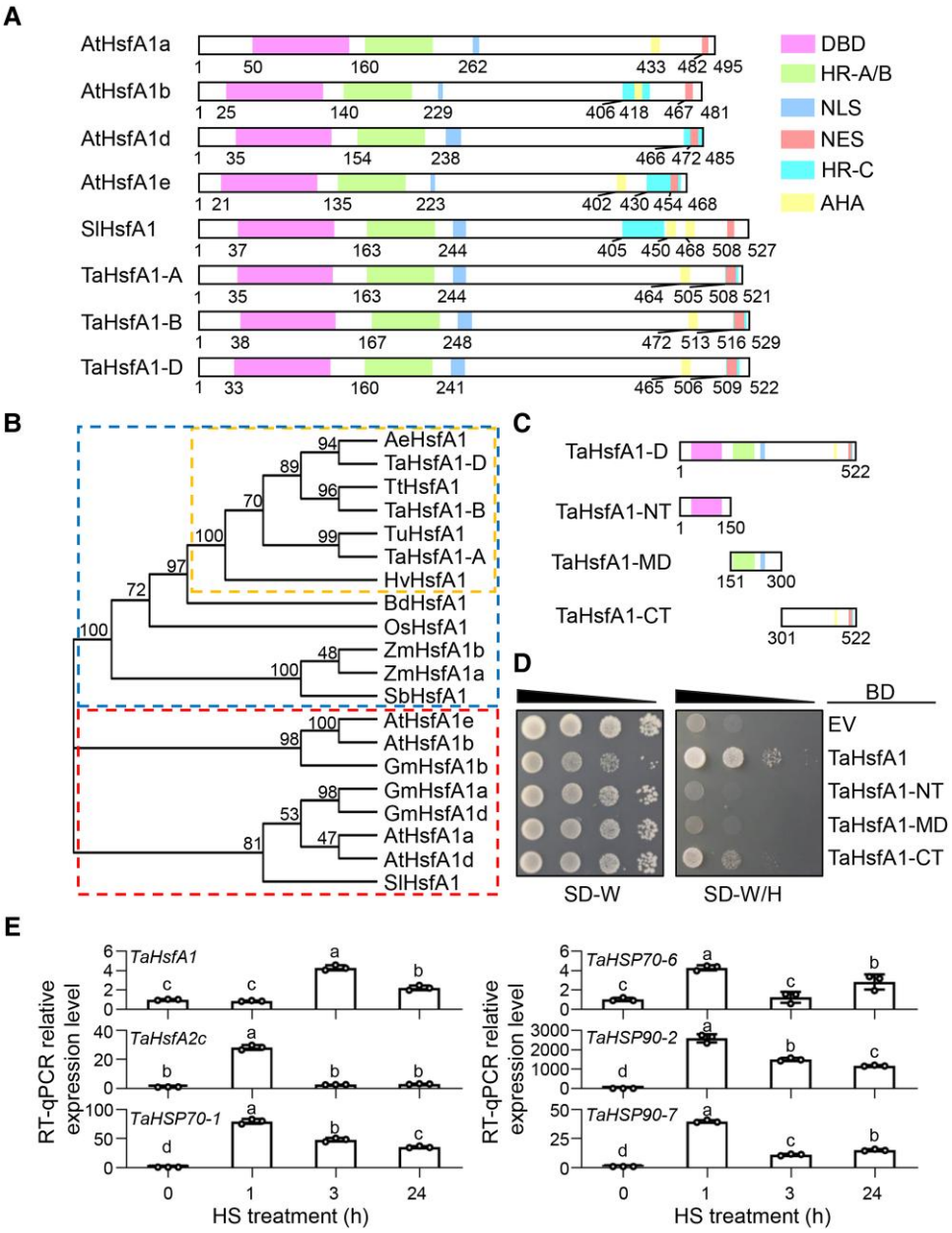

Figure 1. Characterization of HsfA1 proteins in wheat. **A)** Highly conserved domains of HsfA1 proteins from different plant species. Numbers below the boxes indicate the start residues of the motifs. DBD, DNA-binding domain; HR-A/B or HR-C, heptad hydrophobic repeat; NLS, nuclear localization signal; NES, nuclear export signal; AHA, a short activator peptide motif rich in aromatic, hydrophobic, and acidic amino acid residues. **B)** Phylogenetic analysis of HsfA1 proteins from *A. thaliana* (*At*), tomato (*S. lycopersicum*, *Sl*), soybean (*G. max*, *Gm*), sorghum (*S. bicolor*, *Sb*), maize (*Z. mays*, *Zm*), rice (*O. sativa*, *Os*), *B. distachyon* (*Bd*), barley (*H. vulgare*, *Hv*), bread wheat (*T. aestivum*, *Ta*), *T. urartu* (*Tu*), *Triticum turgidum* (*Tt*), and *A. tauschii* (*Ae*). Bootstraps = 1,000. The 3 dotted boxes indicate the HsfA1s from dicotyledons, monocotyledons, and tribe Triticeae, respectively. **C)** Schematic representation of the amino terminal (NT), middle (MD), and carboxyl terminal (CT) truncated versions of TaHsfA1 used for further analysis. **D)** Transcriptional activation activity assay of the full-length and truncated versions of TaHsfA1 in yeast AH109 (*S. cerevisiae*) cells. BD, GAL4 DNA-binding domain. **E)** Transcriptional changes in *TaHsfA1* (including three homologs from the A, B, and D subgenomes) and its downstream regulated genes, including *TaHsfA2c* and 4 *TaHSPs*, in response to HS treatment. Values are means ± SD ($n = 3$). Different letters represent significant differences by 1-way ANOVA with Tukey's multiple comparison test ($P < 0.05$).

subsequent expression in yeast strain AH109 revealed that only full-length TaHsfA1 together with TaHsfA1-CT promoted yeast growth (Fig. 1D). These observations suggest that TaHsfA1 confers transcriptional activation activity, which depends on its CT.

To investigate whether *TaHsfA1* is transcriptionally responsive to heat signals, we treated seedlings of wheat cultivar CS with HS (37 °C) while using seedlings under ambient growth conditions (24 °C) as negative controls and measured the expression of *TaHsfA1* in these samples by reverse

transcription quantitative PCR (RT-qPCR). We also detected transcriptional changes in some well-known HS-responsive genes, including *TaHsfA2c*, *TaHSP70-1*, *TaHSP70-6*, *TaHSP90-2*, and *TaHSP90-7*, which are directly or genetically regulated by TaHsfA1 (Ohama et al. 2017; Castro et al. 2018; Kumar et al. 2020; Ma et al. 2023). HS-responsive gene expression was induced very quickly by HS (within 1 h; Fig. 1E); however, the induction of *TaHsfA1* was much slower than that of its downstream genes (3 h post HS treatment). These findings indicate that TaHsfA1-activated HSRs during HS are likely due to the activity of TaHsfA1 rather than the relatively slow transcriptional induction of the *TaHsfA1* gene itself.

TaHsfA1 is required for thermotolerance in wheat

To evaluate the biological significance of *TaHsfA1* in sensing HS in wheat, we generated *TaHsfA1*-knockout null mutant wheat plants, *Tahsfa1* (lines #1 and #2 with all 3 homoeologs being knocked out), via CRISPR/Cas9–mediated gene editing using the genetic background Fielder (Fig. 2A). When cultivated at 24 °C, the *Tahsfa1* mutants exhibited completely normal phenotypes, suggesting that the loss of *TaHsfA1* does not damage wheat growth. However, when treated with 42 °C for 2 d, followed by recovery at 24 °C for 5 d, most *Tahsfa1* seedlings withered and showed much lower survival rates than the wild-type (WT) controls (Fig. 2, B and C). In addition, HS treatment at the early milk development stage led to thin and shrunken grains in both the WT and *Tahsfa1* lines, but this HS-triggered damage was less severe in the WT than in the *Tahsfa1* lines, as illustrated by significantly higher thousand grain weight (TGW) in WT versus the *Tahsfa1* lines after HS treatment (Fig. 2, D and E).

We also evaluated the acquired thermotolerance of WT and *Tahsfa1* seedlings. When exposed to 42 °C for 2 d, more than 70% of WT seedlings withered, while all *Tahsfa1* seedlings were nonviable. In a parallel treatment, WT and *Tahsfa1* seedlings were first pretreated with 42 °C for 2 h, allowed to recover at 24 °C for 24 h, and treated with 42 °C for 2 d. Phenotypic analysis revealed that, whereas 42 °C pretreatment largely increased the thermotolerance of both WT and *Tahsfa1* seedlings under long-term HS treatment, *Tahsfa1* seedlings exhibited a significantly lower survival rate than WT seedlings (Supplemental Fig. S3). Together, these findings suggest that the loss of *TaHsfA1* largely, but not completely, compromises the basal and acquired thermotolerance of wheat.

HS-responsive genes and signaling pathways regulated by TaHsfA1

To assess the HS-responsive signaling pathways related to *TaHsfA1*, we performed transcriptome profiling by exposing Fielder and *Tahsfa1* (line #1) seedlings to HS (37 °C) for 10 and 30 min, respectively, while untreated seedlings were employed as controls (designated 0 min). By comparing the gene expression levels between the HS-treated and untreated samples following RNA-seq, we identified sets of HS-responsive differentially expressed genes (DEGs) in Fielder and *Tahsfa1* seedlings (Supplemental Data Set 2). In Fielder seedlings, for instance, 6,989 genes were induced, while 4,054 genes were suppressed by HS treatment, while in *Tahsfa1* seedlings, 7,711 and 3,250 genes were up- and downregulated by HS, respectively (Fig. 3, A and B). Notably, the induction of HSP-encoding genes in response to HS was largely attenuated in *Tahsfa1* compared to WT seedlings (Supplemental Fig. S4 and Data Set 3), which is consistent with the finding that TaHsfA1 is a major upstream activator of *HSP* genes.

Gene Ontology (GO) analysis showed that the HS-induced DEGs were specifically enriched in biological processes and molecular functions related to "protein folding," "response to heat," "response to reactive oxygen species," "DNA-binding transcription factor activity," "unfolded protein binding," and "protein dimerization activity," while the downregulated DEGs were enriched in "transmembrane transport" and "transmembrane transporter activity" processes (Supplemental Fig. S5 and Data Set 4). Indeed, these signaling pathways and biological processes are closely related to HSRs in plants (Zhang et al. 2022).

Among the DEGs, 2,137 and 2,300 genes were up- or downregulated, respectively, in the WT but were less sensitive to HS in *Tahsfa1* plants (Fig. 3A). For example, a group of genes (indicated by the dashed black box in Fig. 3B) was dramatically induced by HS in WT seedlings but not in *Tahsfa1* seedlings (Fig. 3, A and B). These DEGs are likely *TaHsfA1* dependent. GO enrichment analysis revealed that these DEGs were significantly enriched in abiotic stress responses, including "protein folding," "response to heat," and "unfolded protein binding" (Figs. 3C and S6A).

In contrast, many genes were more highly induced in *Tahsfa1* seedlings than in WT seedlings (Fig. 3, A and B, indicated by dashed red box). We reasoned that the transcriptional induction of these DEGs may be due to HS-triggered damage caused by the loss of *TaHsfA1*. In support of this notion, GO analysis revealed that most of these DEGs were significantly enriched in pathways related to "response to abscisic acid," "response to wounding," and "responses to water deprivation" (Figs. 3C and S6, B and C).

Next, we carried out RT-qPCR assays to validate the transcriptome profiling data. After the loss of *TaHsfA1*, large groups of genes were unable to respond to HS signals at the transcriptional level, including not only the Hsf genes *HsfA2* and *HsfA6a* and groups of *HSP* genes but also the reactive oxygen species (ROS) detoxification genes *TaAPX3* (*Ascorbate peroxidase 3*) and *TaGST* (*Glutathione-S-transferase*), the abscisic acid (ABA) signal regulating genes *TaPP2C5* (*Protein phosphatase 2C5*) and *TaPP2C12*, the membrane protein encoding genes *TaREM4.2* (*Remorin*) and *TaPDR9* (*Pleiotropic drug resistance 9*), the cell division regulating genes *TaCDC27* (*Cell division cycle 27*) and *TaCYCL1* (wheat homologous gene of Arabidopsis *CYCLIN 1*), and the exocyst

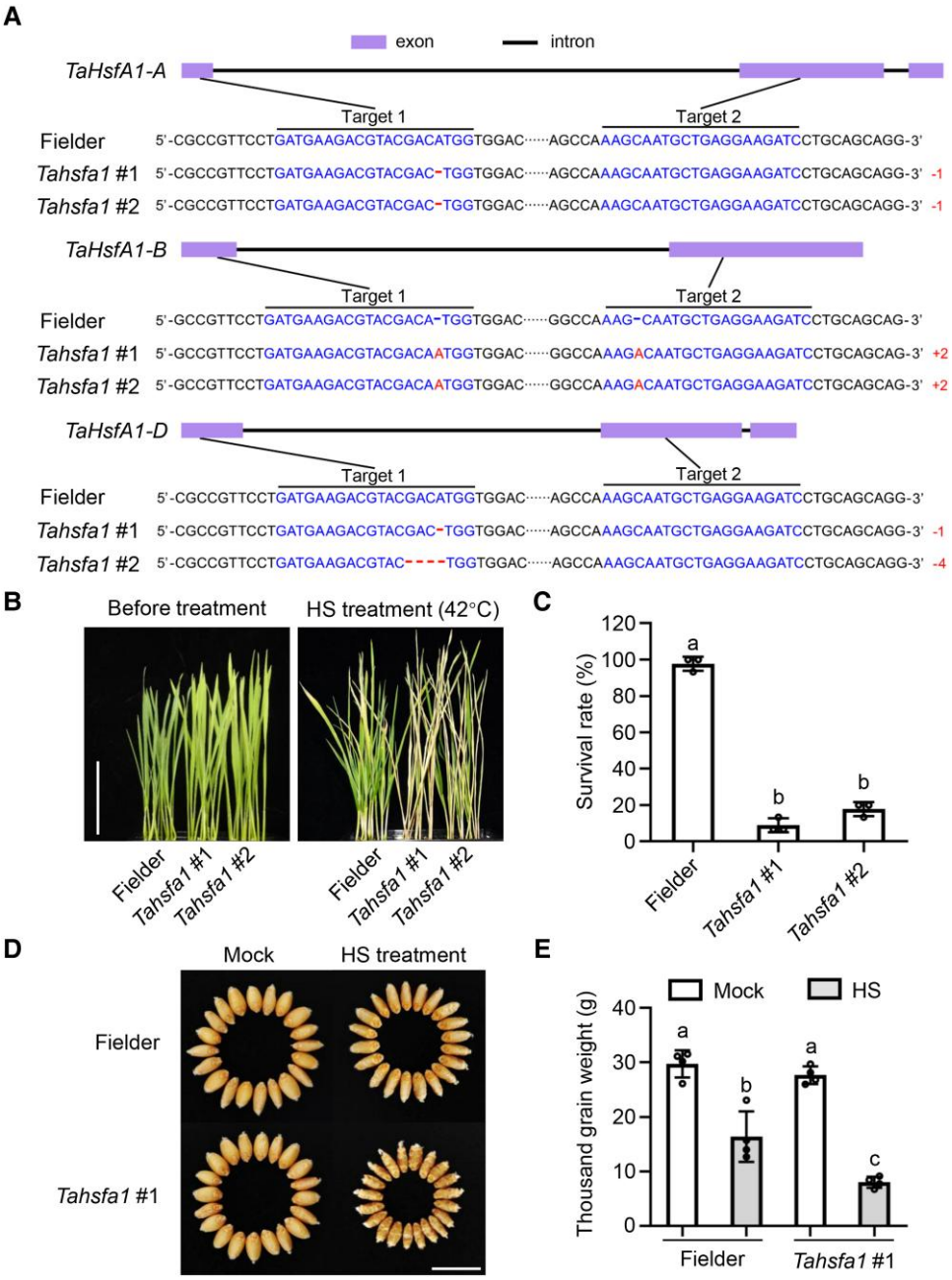

Figure 2. *TaHsfA1* is required for basal heat tolerance in wheat. **A)** CRISPR/Cas9–mediated mutations in the *TaHsfA1-A*, *TaHsfA1-B*, and *TaHsfA-D* genes. The positions of the 2 sites (target 1 and target 2) for CRISPR/Cas9 gene editing are indicated by black lines. The red dashes and letters represent base deletions and insertions, respectively. The numbers of deleted (−) or inserted (+) bases are shown beside the sequences. **B)** Phenotypes of *Tahsfa1* and WT Fielder before and after HS treatment at the seedling stage. Bar, 5 cm. **C)** Statistical analysis of the seedling survival rates shown in **B)**. Data are the means ± SD ($n = 3$). **D)** The grain phenotypes of *Tahsfa1* and Fielder with or without HS treatment. Mock, under normal growth conditions without HS. Bar, 1 cm. **E)** Statistical analysis of the TGW values shown in **D)**. Data are the means ± SD ($n = 4$). Different letters in **C)** and **E)** represent significant differences by 1-way ANOVA with Tukey's multiple comparison test ($P < 0.05$).

subunit-encoding genes *TaEXOC70A1* and *TaEXOC70C1* (wheat homologous genes of Arabidopsis *EXOCYST SUBUNIT EXO70 FAMILY PROTEIN A1* and *EXO70C1*; Figs. 3D, S7, and S8). These findings suggest that *TaHsfA1* broadly participates in multiple biological signaling pathways for the control of thermal tolerance in wheat.

TaHsfA1 is SUMO-modified in a thermosensitive manner

Upon HS perception, TaHsfA1 induces HSRs very quickly before the transcriptional activation of *TaHsfA1* genes (Fig. 1E). Thus, we reasoned that the protein state of TaHsfA1 may play a central role in sensing upstream HS signals. We

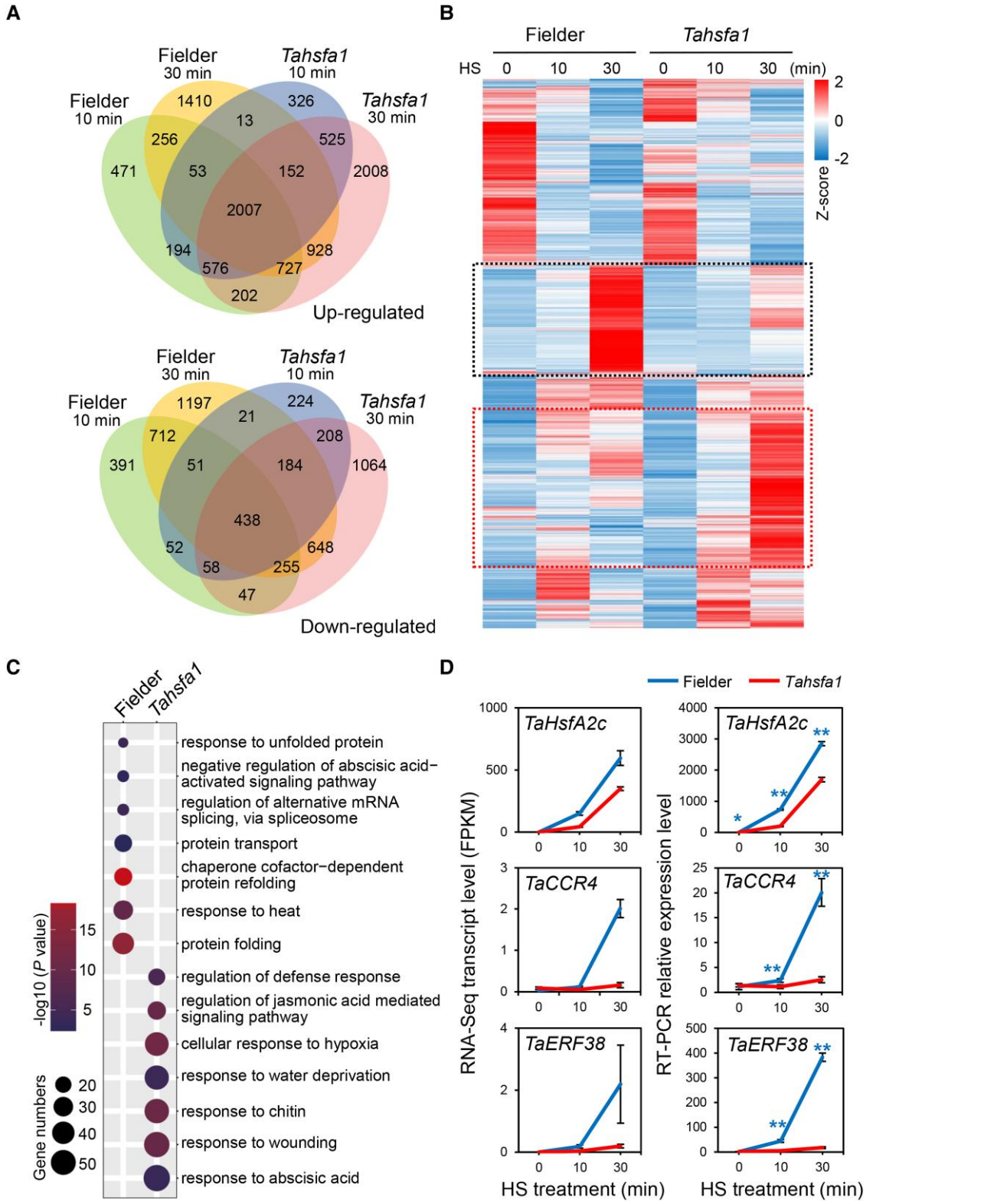

Figure 3. Transcriptome profiling reveals the roles of *TaHsfA1* in regulating wheat thermosensing signaling networks. **A)** Venn diagram showing the numbers of DEGs in response to HS shared between the *Tahsfa1* and WT lines. **B)** Heatmap showing the global transcriptional changes in DEGs before and after HS treatment. The expression value was normalized by *Z*-score. The 2 dashed boxes indicate the DEGs more strongly induced in the Fielder line than the *Tahsfa1* lines and those more highly induced in the *Tahsfa1* lines than in the Fielder line, respectively. **C)** GO enrichment analysis of Fielder-specific and *Tahsfa1*-specific DEGs in response to HS. **D)** RT-qPCR confirming the expression patterns of selected DEGs in Fielder and *Tahsfa1* in response to HS treatment. Asterisks indicate significant differences between the *Tahsfa1* and Fielder lines at the same time point; $^{*}P < 0.05$; $^{**}P < 0.01$ (Student's *t* test). Data are the means ± SD ($n = 3$).

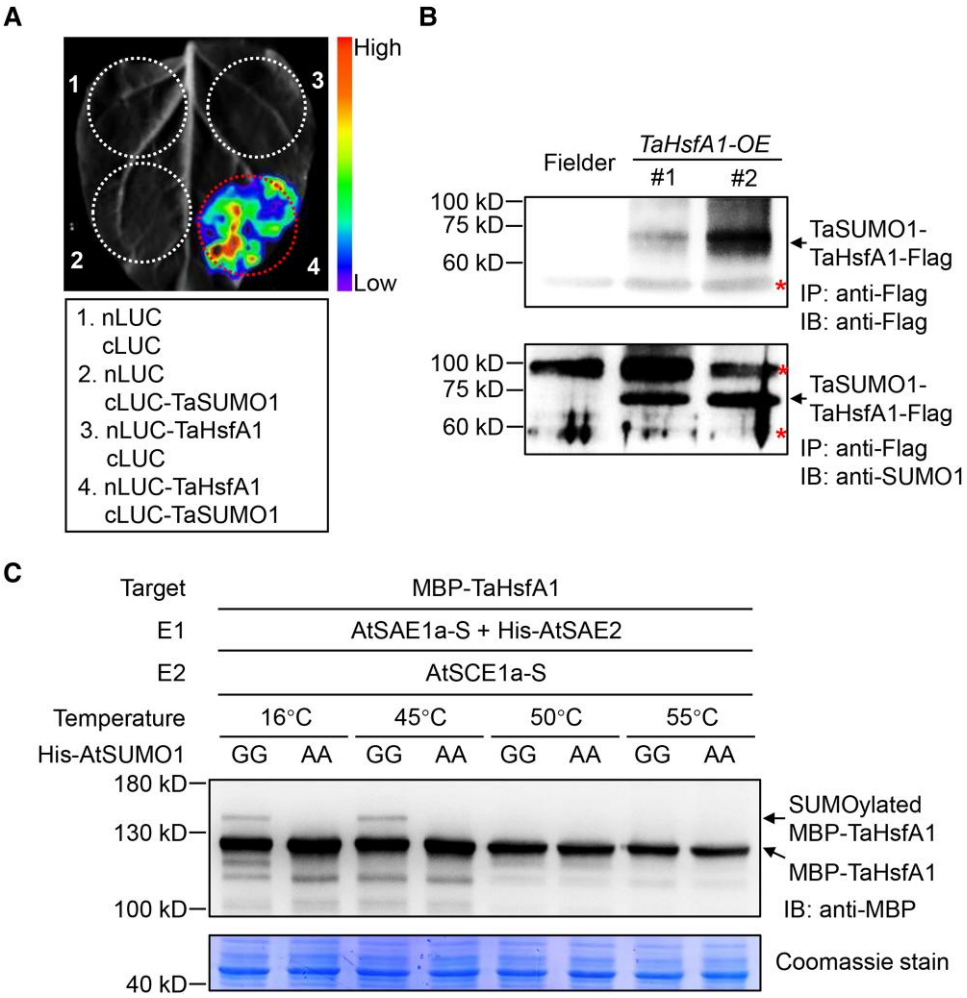

Figure 4. TaHsfA1 is SUMO-modified in a thermosensitive manner. **A)** Split-LCI assay showing the association between TaHsfA1 and TaSUMO1. TaHsfA1-nLUC and cLUC-TaSUMO1 were coexpressed in *N. benthamiana* leaves, and the LUC signal was detected 36 to 48 h post expression. **B)** In vivo immunoprecipitation assay showing that TaHsfA1 is conjugated with TaSUMO1. Transgenic wheat plants overexpressing *TaHsfA1-Flag* (*TaHsfA1-OE*) were employed in the assay, while Fielder plants without transgene integration were used as the negative controls. The asterisks indicate nonspecific shift bands. **C)** In vitro reconstructed SUMOylation assay in *E. coli* cells showing the thermosensitive SUMO modification of TaHsfA1. GG, AtSUMO1 with the C-terminal Gly-Gly sequence exposed; this form can be covalently attached to the target protein; AA, AtSUMO1 with its C-terminal Gly-Gly sequence mutated to Ala-Ala; this form cannot be attached to the target protein. Coomassie blue staining showing the input of total proteins. IB, immunoblotting.

therefore conducted a yeast 2-hybrid (Y2H) assay using TaHsfA1 as a bait to screen candidate proteins that interact with TaHsfA1. Many proteins were identified, including chromatin remodeling protein SPLAYED (SYD), wheat homologous protein of Arabidopsis SODIUM- AND LITHIUM-TOLERANCT 1 (SLT1), and histone acetyltransferase (TaHAG1) (Supplemental Data Set 5). Among these, the SUMO protein TaSUMO1 was of particular interest since previous studies have revealed that SUMOylation plays multiple roles in HSRs (Goodson et al. 2001; Hietakangas et al. 2003; Cohen-Peer et al. 2010). Thus, we selected TaSUMO1 for further analysis (Supplemental Fig. S9A).

The TaHsfA1–TaSUMO1 association in plant cells was validated by a split luciferase (LUC) complementation imaging (split-LCI) assay in *Nicotiana benthamiana* (Fig. 4A) and an in vivo immunoprecipitation assay using transgenic wheat plants overexpressing Flag-tagged *TaHsfA1* (*TaHsfA1-OE*, #1 and #2) (Fig. 4B). To determine whether the TaHsfA1–TaSUMO1 interaction is based on covalent conjugation, we reconstructed a SUMOylation cascade in vitro in *Escherichia coli* BL21 (DE3) cells, where MBP-tagged TaHsfA1 was coexpressed with the Arabidopsis SUMO1 isoform with its C-terminal Gly-Gly sequence exposed ($SUMO1_{GG}$) to check for TaHsfA–SUMO1 conjugation; an inactive $SUMO1_{AA}$ isoform with its C-terminal Gly-Gly mutated to Ala-Ala was employed as the negative control (Okada et al. 2009). Indeed, the molecular weight shift of MBP-TaHsfA1 due to conjugation of SUMO1 was exclusively observed in samples expressing TaHsfA1–$SUMO1_{GG}$ but not in TaHsfA1–$SUMO1_{AA}$ control samples (Fig. 4C), suggesting that TaHsfA1 is SUMO-modified. In

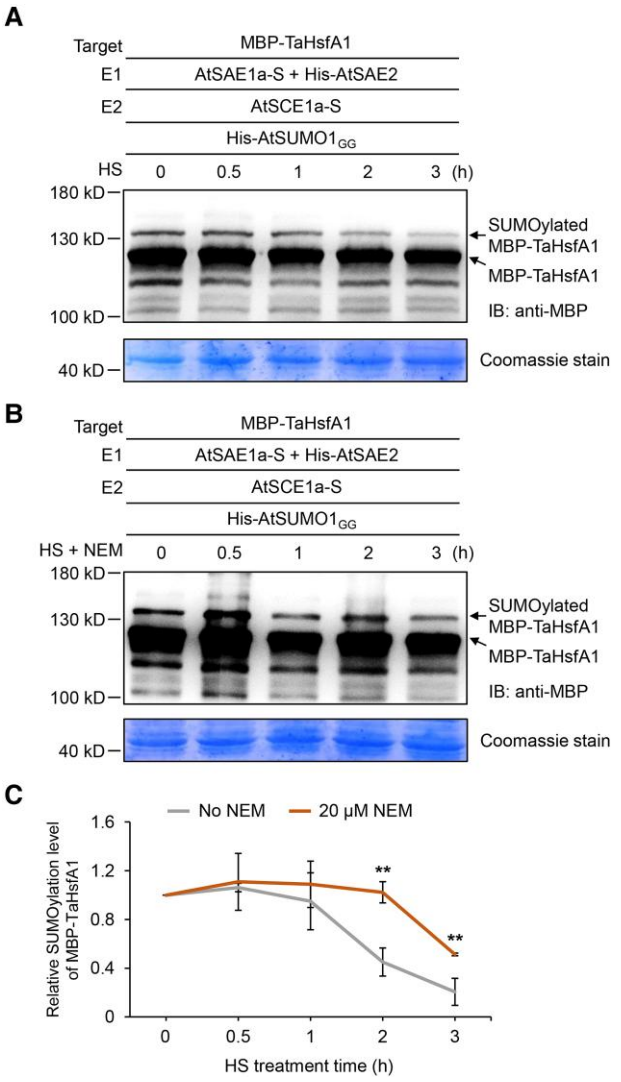

Figure 5. SUMOylation of TaHsfA1 is attenuated by HS treatment. **A)** In vitro reconstructed SUMOylation assay in *E. coli* cells showing that 50 °C HS treatment dampens SUMO1 conjugation of TaHsfA1. **B)** NEM treatment effectively slows the HS-triggered reduction in TaHsfA1 SUMOylation. In **A)** and **B)**, Coomassie blue staining was employed as the input control. IB, immunoblotting. **C)** Quantitative analysis of the relative SUMOylation levels of MBP-TaHsfA1 shown in **A)** and **B)**. Samples without NEM treatment (No NEM) were employed as negative controls. Asterisks indicate significant differences between NEM-treated and untreated cells at the same time point; $^{**}P < 0.01$ (Student's *t* test). Data are the means ± SD ($n = 3$).

support of this notion, our results confirmed a direct interaction between TaHsfA1 and the SUMO E3 ligase TaSIZ1 (Supplemental Fig. S10), pointing to a potential role of TaSIZ1 in mediating TaHsfA1 SUMOylation.

To investigate the potential relationship between SUMO modification and HS in wheat, we checked the overall SUMOylation profiles of wheat proteins at different time points (0.5, 3, and 24 h) during HS treatment. Short-term HS treatment (0.5 h) induced the rapid accumulation of SUMO-conjugated proteins, while after a longer HS treatment (3 to 24 h), the levels of SUMO-conjugated proteins dramatically decreased and ultimately reached a level identical to that of the control sample (0 h; Supplemental Fig. S11). We then examined whether the SUMOylation of TaHsfA1 dynamically changed in response to HS. Similar to that in wheat cells, the in vitro reconstructed SUMOylation assay in *E. coli* cells revealed that TaHsfA1 was indeed SUMO1 conjugated (16 °C). Although this SUMO modification was not influenced by mild high temperatures (such as 45 °C), it was completely abolished by higher temperatures (such as 50 and 55 °C; Fig. 4C).

In a continuous HS treatment assay, we induced the SUMOylation of TaHsfA1 at 16 °C and treated the SUMOylated TaHsfA1 proteins with 50 °C for 3 h. The levels of SUMO1-conjugated TaHsfA1 protein gradually decreased following 50 °C HS treatment (Fig. 5, A and C). *N*-Ethylmaleimide (NEM) is an efficient SUMO protease inhibitor that blocks SUMO removal from SUMOylated proteins by inhibiting SUMO protease activity (Qu et al. 2020). Indeed, NEM application blocked the HS-triggered downregulation of TaHsfA1 SUMOylation (Fig. 5, B and C). Together, these results strongly suggest that TaHsfA1 is SUMO-modified in a thermosensitive manner, while high temperature represses this SUMO modification.

To evaluate the significance of TaHsfA1 SUMOylation in vivo, we examined the HS-induced activation of TaHsfA1-regulated downstream genes in WT and *Tahsfa1* plants at different time points during HS treatment. As expected, all these genes showed higher transcript levels in the WT than in the *Tahsfa1* lines (Fig. 6A). More intriguingly, the transcript levels of these genes peaked at the early stage of HS treatment (within 0.5 to 1 h) but quickly decreased after 1 h of heat exposure and ultimately reached relatively low levels similar to those in the untreated control samples (0 h; Fig. 6A). This transcriptional resilience indicates that the transcriptional activation activity of TaHsfA1 is partly attenuated during prolonged HS treatment (longer than 1 h), and this attenuation is likely related to the reduction in TaHsfA1 SUMOylation in response to HS, as shown in Fig. 5A.

To further explore this notion, we treated WT and *Tahsfa1* wheat seedlings with NEM and again examined the expression patterns of TaHsfA1-regulated downstream genes during HS. The transcript levels of most of the tested genes were enhanced by NEM treatment during HS, especially at 1 to 3 h during HS (Fig. 6B). These findings, together with the reduced levels of TaHsfA1–TaSUMO1 conjugation during sustained HS treatment (Fig. 5A), point to a potential role of TaHsfA1 SUMOylation in regulating the transcriptional activation activity of TaHsfA1 as well regulating downstream HSR.

Lys459 is a key SUMOylation site in TaHsfA1

To identify potential SUMO conjugation residues in TaHsfA1, we used the web-based tools $SUMO_{PLOT}$ (http://www.abgent.com/sumoplot) and JASSA (http://www.jassa.fr/index.php?m=jassa) for SUMOylation site prediction. In total, 7 potential sites (Lys77, Lys98, Lys103, Lys164, Lys175,

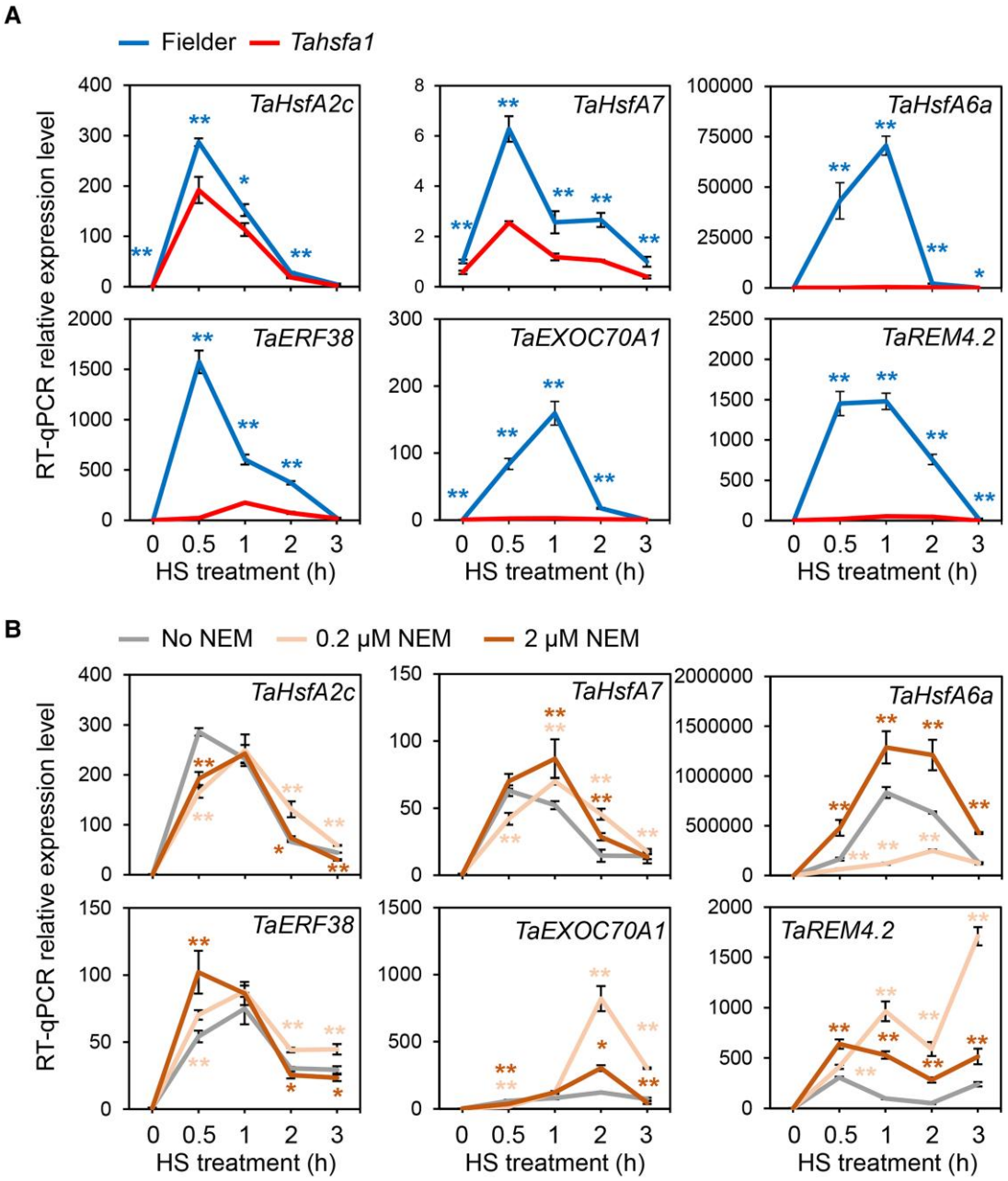

Figure 6. NEM treatment alters the expression patterns of TaHsfA1-regulated downstream genes during HS. **A)** Dynamic changes in TaHsfA1-regulated downstream genes, including *TaHsfA2c*, *TaHsfA7*, *TaHsfA6a*, *TaERF38*, *TaEXOC70A1*, and *TaREM4.2*, in response to HS treatment at different time points. **B)** Transcript levels of TaHsfA1-regulated downstream genes in wheat seedlings in response to NEM and HS treatment. Asterisks indicate significant differences between NEM-treated and control seedlings without NEM treatment (No NEM) at the same time point; $^{*}P < 0.05$; $^{**}P < 0.01$ (Student's *t* test). Data are the means ± SD ($n = 3$).

Lys255, and Lys459) were annotated by $SUMO_{PLOT}$, and 4 sites (Lys98, Lys175, Lys241, and Lys255) were annotated by JASSA (Fig. 7A; hereafter we used K77, K98, K103, K164, K175, K241, K255, and K459 to illustrate these amino acids, respectively).

To experimentally validate these sites, we generated truncated versions of TaHsfA1, i.e. TaHsfA1-NT, TaHsfA1-MD, and TaHsfA1-CT (Fig. 1C), and tested their potential in conjugating with TaSUMO1. Split-LCI assays indicated that TaHsfA1-CT plays a major role in mediating the physical interaction of TaHsfA1 with TaSUMO1 or TaSIZ1 (Supplemental Fig. S12A). We also used an in vitro reconstructed SUMOylation system to identify the domains of TaHsfA1 in conjugation with SUMO and revealed strong SUMOylation signals for TaHsfA1-NT and TaHsfA1-CT but weaker signal for TaHsfA1-MD (Fig. 7B).

To identify the exact residues responsible for SUMO modification, we introduced amino acid substitutions to replace

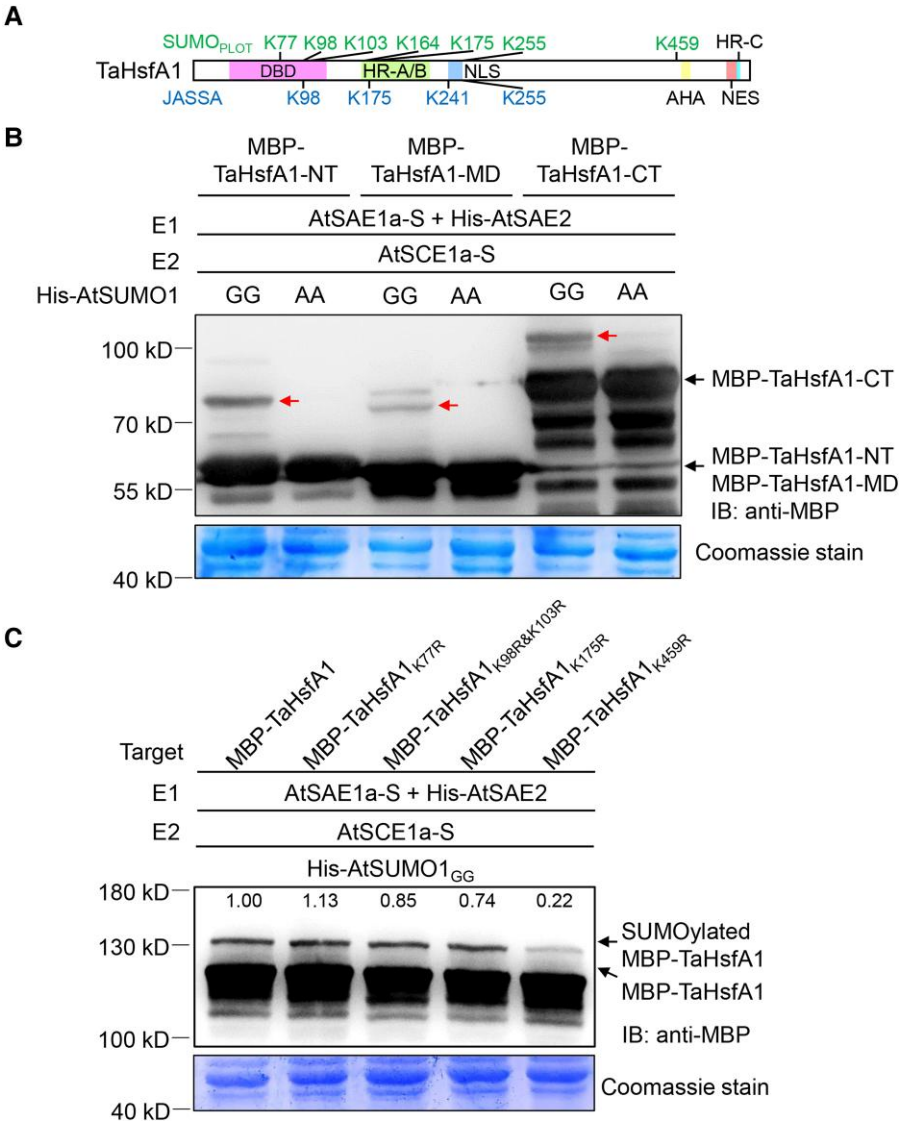

Figure 7. Lys459 is a major SUMO conjugation site in TaHsfA1. **A)** Schematic representation of the predicted SUMOylation sites in TaHsfA1. Positions of potential sites predicted by SUMO$_{PLOT}$ are shown above the shematic diagram, while the residues annotated by JASSA are indicated below the diagram. The amino acid sites of Lys77, Lys98, Lys103, Lys164, Lys175, Lys241, Lys255, and Lys459 were represented by K77, K98, K103, K164, K175, K241, K255, and K459, respectively. **B)** In vitro reconstructed SUMOylation assay in *E. coli* cells showing that all 3 truncated versions of TaHsfA1 were modified by AtSUMO1$_{GG}$ and that TaHsfA1-MD had the lowest SUMOylation level. Red arrows indicate SUMOylated MBP-TaHsfA1-NT, SUMOylated MBP-TaHsfA1-MD, and SUMOylated MBP-TaHsfA1-CT. **C)** In vitro reconstructed SUMOylation assay in *E. coli* cells showing that only the Lys459 to Arg (K459R) mutation substantially blocked TaHsfA1–SUMO1 conjugation. The experiment was performed 3 times with the same results. IB, immunoblotting. Coomassie staining was used to check the input proteins in **B)** and **C)**.

the predicted SUMO-modified Lys residues in the NT, MD, and CT regions of TaHsfA1 with arginine (Arg; R for short) and generated 4 different mutated versions of full-length TaHsfA1: TaHsfA1$_{K77R}$ harboring the K77-to-R mutation, TaHsfA1$_{K98R&K103R}$ harboring both the K98-to-R and K103-to-R mutations, TaHsfA1$_{K175R}$ harboring the K175-to-R mutation, and TaHsfA1$_{K459R}$ harboring the K459-to-R mutation. A SUMOylation assay in *E. coli* cells revealed that only the K459R mutation strongly attenuated SUMO1 conjugation on TaHsfA1 (Figs. 7C and S12B). This result was further validated by a split-LCI assay in which the K459R mutation significantly reduced the LUC signal of the TaHsfA1–TaSUMO1 association (Supplemental Fig. S12C). Together, these results support the notion that K459 is a major residue in TaHsfA1 responsible for SUMO modification.

Notably, the K459 residue is only evolutionarily conserved in rice, *Brachypodium distachyon* and tribe Triticeae crop plants (Supplemental Fig. S9B), while it is divergent in the monocots maize (*Zea mays*) and sorghum (*Sorghum bicolor*) and in dicots, with the exception of HsfA1b from Arabidopsis and soybean (*Glycine max*). Based on these findings, coupled with the results of phylogenetic analysis showing that rice, *B.*

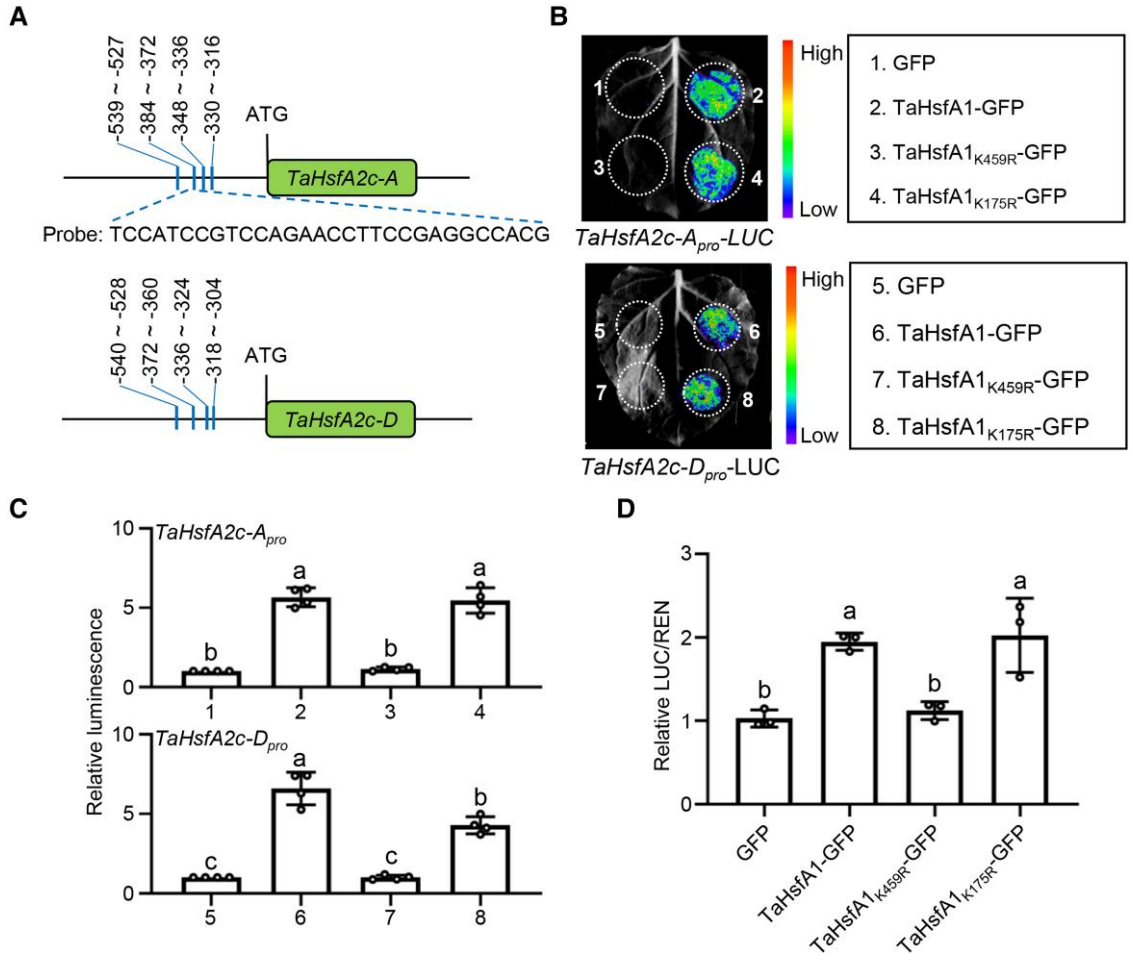

Figure 8. The K459R mutation abolishes the transcriptional activation of TaHsfA1. **A)** Schematic representation of the *TaHsfA2c-A* and *TaHsfA2c-D* promoters. The boxes represent the gene coding regions, and the vertical lines indicate putative HSE motifs located in the promoter regions. The numbers above the HSEs indicate the positions of these HSEs relative to the ATG start codon. The probe sequence used for the EMSA is shown below. **B, C)** Transient transcriptional activation activity assays showing that TaHsfA1 harboring the K459R point mutation ($TaHsfA1_{K459R}$) fails to activate the transcription of its targeted gene, *TaHsfA2c*. Representative images are shown in **B)**, while statistical quantifications of relative luminescence intensities are shown in **C)**. Data are means ± SD ($n = 4$). **D)** Transient transcriptional activation activity assay in wheat protoplasts confirming that $TaHsfA1_{K459R}$ fails to activate *TaHsfA2c*. Data are means ± SD ($n = 3$). One-way ANOVA and Tukey's multiple comparison test were used for significance analysis. Different letters above the boxes represent significant difference ($P < 0.05$).

distachyon, and tribe Triticeae HsfA1s share higher levels of sequence similarity compared to those from other monocots and dicots (Fig. 1B), we propose that the positive selection and fixation of the HsfA1-K459 residue was an evolutionarily recent event that specifically occurred in a portion of monocot crops.

TaHsfA1 confers transcriptional activation activity depending on its intact K459 residue

TaHsfA1 behaves as a transcriptional activator to facilitate downstream gene expression. To confirm this notion, we carried out transient transcriptional activity assays in *N. benthamiana*. Indeed, TaHsfA1 activated the luminescence intensity of *TaHsfA2c-A_{pro}-LUC* and *TaHsfA2c-D_{pro}-LUC* reporters (driven by the native promoters of the *TaHsfA2c-A* and *TaHsfA2c-D* genes, respectively; Figs. 8A and S13), suggesting that TaHsfA1 has strong transcriptional activation activity. However, when we substituted Arg (R) for the K459 residue in TaHsfA1 to block in vitro SUMOylation at this site, the mutated $TaHsfA1_{K459R}$ was unable to activate the *TaHsfA2c-A_{pro}-LUC* and *TaHsfA2c-D_{pro}-LUC* reporters (Fig. 8, B and C). To rule out the possibility that the K-to-R substitution leads to nonspecific results due to changes in TaHsfA1 protein properties, we employed $TaHsfA1_{K175R}$ as a negative control. As expected, $TaHsfA1_{K175R}$, largely resembling WT TaHsfA1, conferred strong transcriptional activation activity (Fig. 8, B and C).

We also performed a transient transcriptional activation activity assay in wheat protoplasts to further validate the effect of the K459R mutation on TaHsfA1 protein function. In this assay, we generated a *TaHsfA2c-A_{pro}-LUC/35S_{pro}-REN*

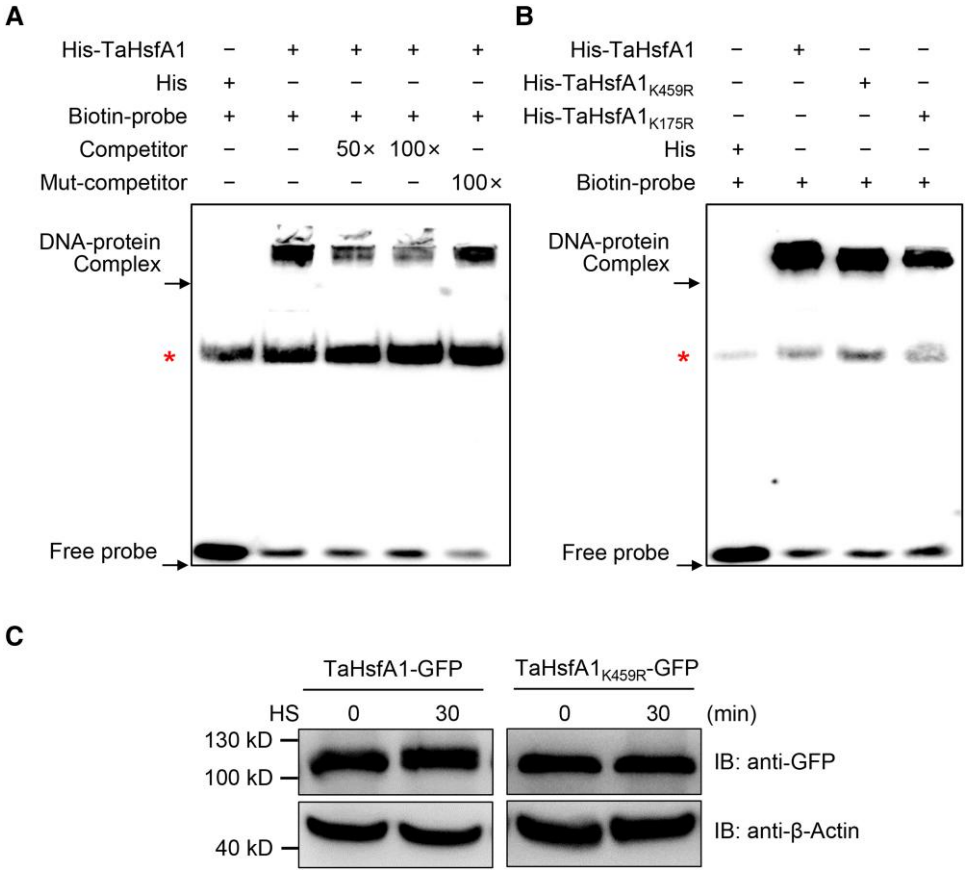

Figure 9. The K459 mutation does not influence the DNA-binding activity or protein stability of TaHsfA1. **A)** EMSA revealing that TaHsfA1 directly binds to the promoter region of *TaHsfA2c-A*. **B)** EMSA confirming that the K459R mutation does not influence the association of TaHsfA1 with the *TaHsfA2c-A* promoter. Asterisks in **A)** and **B)** indicate nonspecific binding signals. **C)** Protein accumulation of TaHsfA1-GFP and TaHsfA1$_{K459}$-GFP before and after HS treatment. IB, immunoblotting.

vector as a reporter and coexpressed it with TaHsfA1-GFP, TaHsfA1$_{K459R}$-GFP, and TaHsfA1$_{K175R}$-GFP, respectively, in wheat protoplasts. Quantification of relative LUC/REN reporter activity revealed that the expression of TaHsfA1-GFP and TaHsfA1$_{K175R}$-GFP significantly enhanced LUC activity, while this LUC activation was not observed in TaHsfA1$_{K459R}$-GFP–expressing samples, suggesting that the K459R mutation dampens the transcriptional activation activity of TaHsfA1 in wheat cells (Fig. 8D).

Notably, K459 is located adjacent to the highly conserved AHA motif, which is essential for the transcriptional activation activity of Hsfs (Fig. 7A) (Döring et al. 2000; Kotak et al. 2004), which may further explain the essential role of K459 in modulating the transcriptional activation activity of TaHsfA1. In vitro electrophoretic mobility shift assays (EMSAs) and in vivo protein quantification assays confirmed that the K459R mutation did not alter the DNA-binding activity or protein stability of TaHsfA1 (Fig. 9). Together, these findings support the notion that the K459 residue is required for the transcriptional activation activity of TaHsfA1 and that mutating this residue abolished the ability of TaHsfA1 to regulate downstream gene expression.

TaHsfA1 interacts with the histone acetyltransferase TaHAG1 in a thermosensitive manner

Our Y2H screening assay also identified TaHAG1, a histone acetyltransferase that is homologous to Arabidopsis GENERAL CONTROL NONDEREPRESSIBLE 5 (GCN5), as a candidate protein that interacts with TaHsfA1. Because histone acetyltransferase is widely considered to be a major player in facilitating the transcriptional activation activities of transcription factors by promoting histone acetylation (Supplemental Data Set 5) (Jenuwein and Allis 2001; Lin et al. 2022), we reasoned that this TaHsfA1–TaHAG1 interaction might be involved in the transcriptional activation activity of TaHsfA1. By performing split-LCI and coimmunoprecipitation (Co-IP) assays, we validated the TaHsfA1–TaHAG1 interaction in plant cells (Fig. 10, A and B).

Surprisingly, split-LCI assays revealed that the TaHsfA1–TaHAG1 interaction was also thermosensitive and was considerably weakened by HS treatment (Fig. 10C). Moreover, the K459R point mutation, in contrast to the K175R point mutation, significantly dampened the physical interaction between TaHsfA1 and TaHAG1 (Fig. 10D), indicating that the

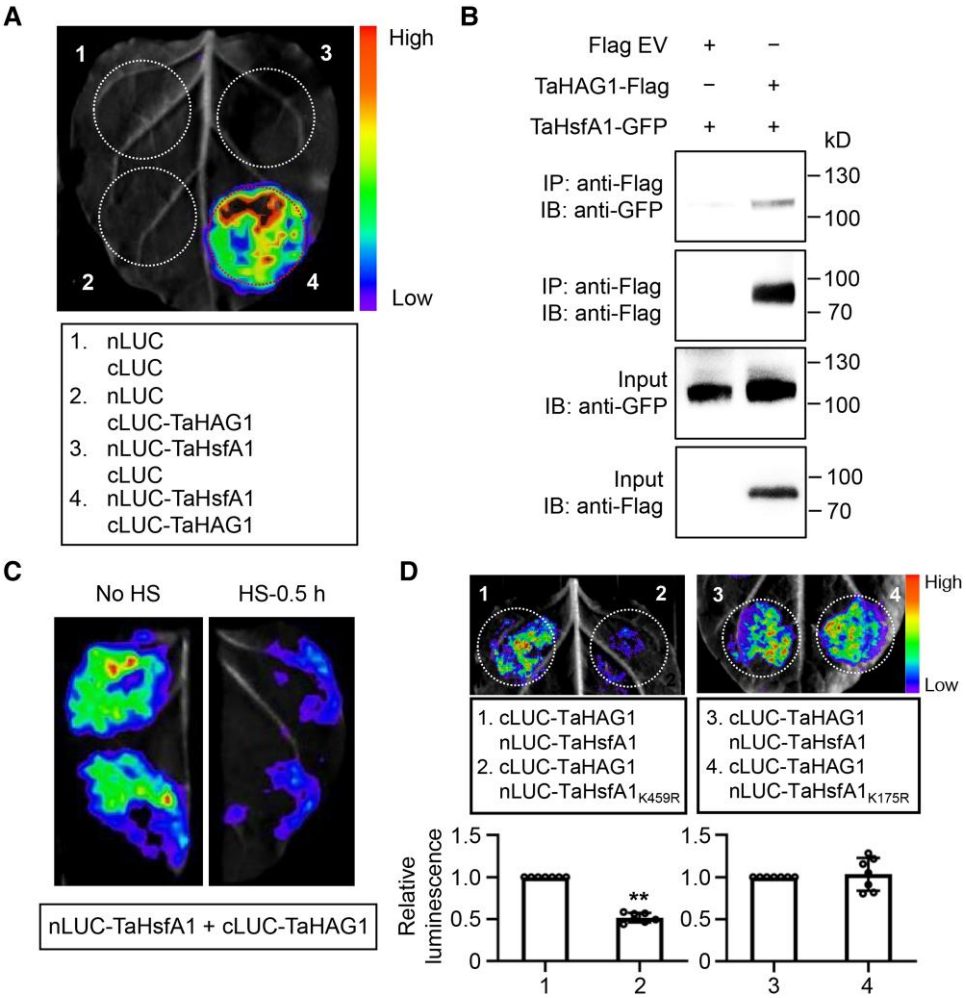

Figure 10. TaHsfA1 interacts with the histone acetyltransferase TaHAG1 in a thermosensitive manner. **A)** Split-LCI assay showing the interaction between TaHsfA1 and TaHAG1. **B)** Co-IP assay revealing the interaction between TaHsfA1 and TaHAG1. The proteins were immunoprecipitated by anti-Flag–conjugated M2 magnetic beads and detected by anti-Flag and anti-GFP antibodies. Flag EV represents the *pCAMBIA1300-Flag* empty vector, which was employed as a negative control. IB, immunoblotting. **C)** Split-LCI assay showing that the interaction between TaHsfA1 and TaHAG1 is largely attenuated by HS treatment. No HS represents the control samples without HS treatment. **D)** Split-LCI assay showing that the K459R mutation in TaHsfA1 hinders its interaction with TaHAG1. Data are means ± SD ($n = 7$). The relative luminescence values in combinations 1 and 3 were set to 1; **significant difference compared to combination 1 at $P < 0.01$ (Student's t test).

intact K459 of TaHsfA1 is essential for the recruitment of TaHAG1.

Interestingly, TaHAG1 also interacts with TaSUMO1, and similar interaction signals were detected between TaHAG1–$TaSUMO1_{GG}$ and TaHAG1–$TaSUMO1_{AA}$ (Supplemental Fig. S14). In addition to the TaHAG1–TaHsfA1 association, we also tested the physical interactions of TaHsfA1 with TaMed18 and TaMed25, the Mediator subunits that bridge RNA polymerase II (Pol II) and transcription factors for transcriptional activation (Zhai and Li 2019). Although strong interactions of TaHsfA1–TaMed18 and TaHsfA1–TaMed25 were detected, they were not influenced by the K459R mutation (Supplemental Fig. S15). Together, these findings confirm the notion that TaHsfA1 recruits the histone acetyltransferase TaHAG1 and the Mediator complex to establish its transcriptional activation activity, while the thermosensitive recruitment of TaHAG1 by TaHsfA1 may further explain the dynamic changes in TaHsfA1 activity in regulating HSRs.

Discussion

Previous studies have identified *TaHsfA1* genes in wheat via bioinformatic and phylogenetic analyses (Xue et al. 2014; Duan et al. 2019). In this study, we systematically analyzed the biological significance of *TaHsfA1* in conferring thermotolerance in wheat. As in other plant species, *TaHsfA1* is a constitutively expressed *Hsf* gene in wheat; its expression was not induced at the early stage of HS (within 1 h of HS treatment) but was only marginally induced at a relatively late stage of HS (after 3 h of HS treatment; Fig. 1E). Notably, TaHsfA1-targeted genes, including *TaHsfA2c* and *HSPs*, were dramatically upregulated at the early stage of

HS (1 h of HS treatment) but restored to normal levels at 3 h of HS treatment (Fig. 1E). The noncorrelated expression patterns of *TaHsfA1* with its target genes suggest that *TaHsfA1* must sense the HS signal for the activation of HSRs via the allostery of its encoded proteins rather than through its HS-induced transcriptional changes. In fact, modifying the activity of a regulatory protein in response to transient environmental changes is thought to be a quicker and more efficient strategy than transcriptional activation (Seo et al. 2012; Zhang et al. 2017; Qin et al. 2022).

The transcription factor TaHsfA1 contains a DBD at its N-terminus for DNA binding and an AHA domain at its C-terminus for transcriptional activation (Fig. 1A). Transient expression assays in yeast confirmed that the transcriptional activation activity of TaHsfA1 is indeed conferred by TaHsfA1-CT (Fig. 1, C and D). As expected, large sets of HS-inducible genes were no longer effectively induced by HS in *Tahsfa1* plants (Fig. 3B). In particular, most of the *HSP* genes were less effectively induced in *Tahsfa1* plants than in WT plants (Supplemental Fig. S4). These results suggest that the loss of *TaHsfA1* leads to the partial attenuation of HSRs. More importantly, the *Tahsfa1* mutant lines were sensitive to HS in terms of seedling establishment and grain filling (Fig. 2, B and E). These transcriptome profiling and phenotyping data support the notion that *TaHsfA1* is a key regulatory gene that contributes to the HSRs and basal thermotolerance of wheat.

Consistent with these findings in wheat, HsfA1a from tomato has also been defined as a master regulator of HSRs, since its unique function in triggering HSRs is not replaced by any other Hsf family members (Mishra et al. 2002). However, Arabidopsis exhibits much higher complexity in sensing HS and contains 4 *HsfA1* genes, *A1a*, *A1b*, *A1d*, and *A1e*, whose biological functions are partially redundant. Thus, Arabidopsis mutants with single or double knockout of *HsfA1s* exhibit no marked defects in HSRs or thermotolerance (Liu et al. 2011; Scharf et al. 2012). Instead, a quadruple mutant (*QK*) with all 4 *HsfA1s* simultaneously knocked out showed dramatically impaired thermotolerance (Liu et al. 2011). Notably, *QK* also exhibited dramatic growth retardation even under nonstress conditions, suggesting that Arabidopsis *HsfA1s* are essential for plant growth and development in addition to their major roles in thermotolerance (Liu et al. 2011). Unlike in Arabidopsis, the *TaHsfA1* null mutation led to no growth defects in wheat (Figs. 2, B and D, and S3). These observations indicate that *HsfA1* genes play highly divergent roles among different plant species.

It is worth mentioning that the loss of *TaHsfA1* failed to completely abolish HSRs, since global transcriptional changes in response to HS were still obvious in the *Tahsfa1* mutant (Figs. 3, B and D, and S4), pointing to much more complex HSR signaling networks in wheat. Considering that there are more than 80 *Hsf* genes in the wheat genome (Duan et al. 2019), it is reasonable to speculate that these *Hsf* genes genetically interact with each other and act redundantly in triggering HSRs in wheat. As a consequence, the HSRs of *Tahsfa1* mutants are partially intact due to the presence of other *Hsf* genes. In addition, some other uncharacterized *Hsf*-independent signaling pathways may also exist to perceive elevated temperatures and initiate downstream HSRs without the need for *TaHsfA1* genes. Indeed, a recent study in Arabidopsis revealed that the circadian clock proteins REVEILLE4 (RVE4) and RVE8 play important roles in regulating early HS-induced gene expression in the absence of HsfA1s, suggesting a plausible alternative for sensing HS and regulating HSRs in addition to canonical HsfA1 signaling (Li et al. 2019). However, whether this RVE4/8 regulon is conserved in monocotyledonous plants such as wheat needs to be further investigated.

In a Y2H screen, TaHsfA1 interacted with TaSUMO1, and this interaction was further confirmed in plant cells (Fig. 4 and Supplemental Data Set 5). The in vivo immunoprecipitation and in vitro SUMOylation assays demonstrated that TaHsfA1–TaSUMO1 conjugation is based on covalent attachment (Fig. 4C). Web-based prediction showed that 8 lysine residues (K77, K98, K103, K164, K175, K241, K255, and K459) in TaHsfA1 are potential SUMOylation sites (Fig. 7A). Notably, based on web-based prediction, the K175 residue has the highest prediction score and is thought to be a canonical and highly confident SUMOylation site (Supplemental Fig. S9B). Unexpectedly, by performing domain truncation and point mutation, we revealed that the nontypical residue K459, with a lower prediction score than the canonical K175, is responsible for SUMO modification in TaHsfA1 (Figs. 7C and S12, B and C). Notably, although strong and relatively weaker SUMOylation signals were separately observed at the NT and MD of TaHsfA1, mutating the K residues in these regions, including K77, K98, K103, and K175, failed to block the SUMOylation of TaHsfA1 (Fig. 7, B and C), suggesting that other SUMOylation sites might exist in these regions, which is worth further investigation.

Previous studies have reported that only 60% of SUMOylation sites conform to the Ψ-K-X-D/E consensus motif, and the others display little sequence similarity (Miller et al. 2010; Rytz et al. 2018). The K459 site in TaHsfA1 likely represents such a noncanonical SUMO conjugation site. Moreover, the SCE1 E2 enzyme is thought to assist in the recognition of the consensus SUMO attachment sites, while SIZ1 usually facilitates SUMO conjugation on highly divergent target sites with little sequence or functional homology (Augustine and Vierstra 2018; Rytz et al. 2018). Indeed, we revealed that TaHsfA1 could directly interact with TaSIZ1, indicating a potential role of TaSIZ1 in triggering TaHsfA1 SUMOylation. In addition, K459 exhibits a lower conservation level than K175 among monocot and dicot plants (Supplemental Fig. S9B), indicating that this K459 SUMOylation site in TaHsfA1 likely evolved recently and could be considered a species-specific molecular mechanism underlying the control of HsfA1 protein activity in select monocot crop plants. However, it should be noted that the in vivo biological significance of this K459 site in controlling TaHsfA1 activity remains to be elucidated, since our current

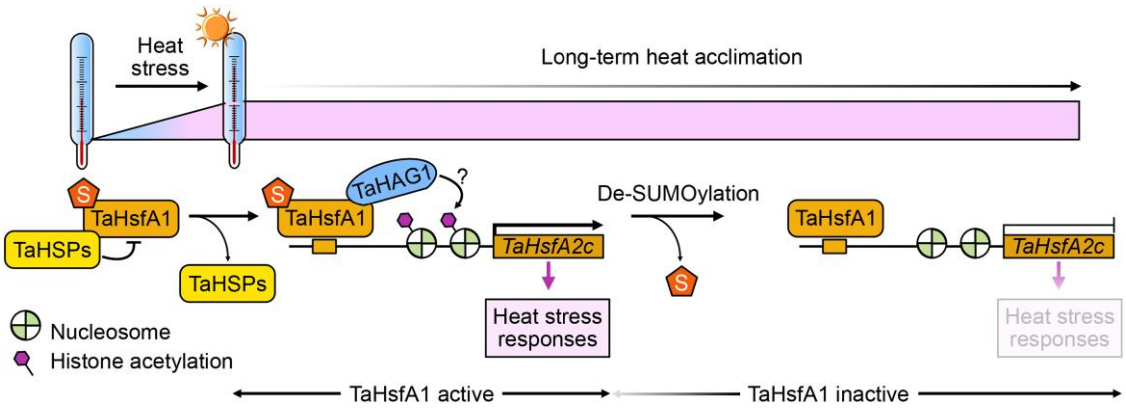

Figure 11. A simplified working model illustrating the TaHsfA1 cycle in response to HS. We propose that the protein activity of TaHsfA1 is tightly controlled by its SUMOylation state: In response to the first wave of HS, SUMOylated TaHsfA1, representing a fully active form, can rapidly bind to downstream genes for transcriptional activation; under relatively long-term HS, the SUMOylation of TaHsfA1 will be largely suppressed, which attenuates TaHsfA1 activity and compromises downstream HSRs, defining a thermosensitive "active-to-inactive" switch of TaHsfA1 and transcriptional adaptation to HS environments.

conclusions are based on transient or in vitro assays. Introgression of a mutant *TaHsfA1*$_{K459R}$ gene copy into *Tahsfa1* wheat mutant plants might further our understanding of the contribution of K459 to TaHsfA1 function.

SUMO modification of substrate proteins is a dynamic and reversible process that involves deSUMOylating proteases (DSPs). To date, a large number of DSPs have been identified in nonplant and plant models, such as SENP1/2/3/6/7 in human, ULP1/2 in yeast, or ESD4, ELS1/2, and ASP1 in Arabidopsis (Pinto et al. 2012; Kong et al. 2017; Castro et al. 2018; Morrell and Sadanandom 2019). Intriguingly, some of these DSPs were validated to be intrinsically temperature-sensitive or important for the adaptation of cells to environmental temperature changes (Pinto et al. 2012; Kong et al. 2017). In this study, we demonstrated that the levels of SUMOylation of TaHsfA1 were considerably reduced under long-term HS treatment, while this SUMO removal was partly attenuated by the application of the SUMO protease inhibitor NEM (Fig. 5). These findings indicate that in wheat, some currently uncharacterized SUMO proteases must exist to complete the thermal-sensitive HsfA1 cycle, which might be crucial for the adaptation of wheat to long-term HS.

Notably, the K459 SUMOylation residue of TaHsfA1 is located at the flanking region of the AHA motif, pointing to a potential role of SUMO conjugation in regulating the transcriptional activation activity of TaHsfA1. As expected, the K459R mutation blocking SUMO conjugation at K459 considerably compromised the transcriptional activation activity of TaHsfA1, while this K459R mutation had no effect on the DNA-binding activity or protein stability of TaHsfA1 (Figs. 8 and 9). Thus, K459 SUMOylation is likely essential for the activity of TaHsfA1 in facilitating downstream gene expression in response to a short bout of HS. However, blocking SUMOylation at this site (as illustrated by TaHsfA1$_{K459R}$) largely sequestered TaHsfA1 activity, thereby leading to transcriptional resilience of HS-responsive genes during long-term HS. Based on these observations, we propose that the dynamic "SUMOylation/deSUMOylation" of TaHsfA1 defines an "ON/OFF" molecular switch for the fine-tuning and timely attenuation of TaHsfA1 activity and HSRs, which is likely important for plant adaptation to prolonged HS (Fig. 11).

The activity of transcription factors in facilitating downstream gene expression depends on the general components involved in modulating epigenetic states and transcriptional events (Chen et al. 2022). In this study, we confirmed that TaHsfA1 recruits the histone acetyltransferase TaHAG1 (Fig. 10). Previous studies have revealed that HAG1 plays a positive role in plant thermotolerance predominantly by mediating the acetylation of histones H3 and H4 and consequent transcriptional derepression of HS-responsive genes during heat exposure (Hu et al. 2015; Zheng et al. 2019; Dong et al. 2021; Lin et al. 2022). In support of this notion, the loss of *TaHAG1* in wheat or the loss of *AtHAG1* in Arabidopsis largely abolished basal heat tolerance (Hu et al. 2015; Lin et al. 2022). In particular, the loss of *HAG1* attenuated the activation of HsfA1-targeted downstream genes, including *HsfA2* and *HsfA3*, during HS treatment but did not affect the expression pattern of *HsfA1* (Hu et al. 2015). This is consistent with our finding that TaHAG1 interacts with TaHsfA1 at the protein level to modulate downstream HSRs (Fig. 10). Moreover, the recruitment of TaHAG1 by TaHsfA1 is not only thermosensitive but also K459-dependent (Fig. 10D). This observation, together with the finding that TaHAG1 also interacts with TaSUMO1 (Supplemental Fig. S14), suggests that the thermosensitive SUMOylation of TaHsfA1 at K459 is essential for the recruitment of this protein via the direct interaction between TaHAG1 and TaSUMO1. However, more evidence is needed to support this hypothesis.

Materials and methods

Plant materials and heat treatment

The transformable bread wheat (*T. aestivum*) cultivar Fielder was used as the material for gene transformation. For gene cloning, genomic DNA or RNA was extracted from spring wheat variety CS. The wheat materials were grown either in 1/4 Hoagland solution (NSP1020, Coolaber) in a growth chamber with 60% relative humidity and 3,000 lx light intensity (Master GreenPower CG T 400W E40; Philips) or in pots with soil in a greenhouse under cycle of 16 h of light at 24 °C and 8 h of dark at 20 °C.

Wheat plants at the first leaf unfolded (Zadoks stage 11) and caryopsis water ripe (Zadoks stage 71) stages were separately selected for HS treatment (Zadoks et al. 1974). To treat seedlings, wheat seeds were washed with 10% sodium hypochlorite solution and deionized water, placed on soaked sprouting paper, transferred to a 4 °C refrigerator, and incubated for 72 h. After being transferred to 25 °C and incubated for 24 h, the germinated seedlings were transferred to Hoagland solution in a growth chamber. Seven-day-old seedlings were exposed to 42 °C high temperature for 2 d, transferred back to 24 °C, and incubated for 5 d. To treat wheat plants at the heading stage, 5 d after flowering, plants in pots were moved to a growth chamber under a cycle of 16 h of light at 35 °C and 8 h of dark at 30 °C. When anthesis was completed, the plants were grown under the same conditions for another 15 d and transferred back to 24 °C for grain harvest.

To analyze acquired thermotolerance, 7-d-old seedlings were acclimated at 42 °C for 2 h and recovered at 24 °C for 24 h, followed by HS treatment at 42 °C for 2 d. The treated seedlings were grown at 24 °C for another 7 d and photographed. For overall SUMOylation profiling, 7-d-old seedlings grown in soil were exposed to 42 °C, and their first leaves were collected at the indicated time points for testing. For NEM treatment, NEM was added to the growth medium of 7-d-old seedlings in a hydroponic box, followed by incubation at 12 h before 42 °C HS treatment. The first leaves were collected for RT-qPCR of related genes. Samples without NEM treatment (No NEM) were employed as control plants.

Genetic transformation

To generate *TaHsfA1*-overexpressing (*TaHsfA1-OE*) transgenic plants, the full-length coding sequence (CDS) of *TaHsfA1-D* fused with the 3 × Flag tag sequence was cloned into the *Age*I/*Hpa*I-digested *PLC41-Z2* vector to generate Ubi_{pro}-*TaHsfA1-D-Flag*, which was further transformed into the wheat variety Fielder via *Agrobacterium tumefaciens*–mediated gene transformation (Kumar et al. 2019). The *PLC41-Z2* expression vector was kept by our own laboratory.

The *Tahsfa1* mutant plants (lines #1 and #2) were generated by CRISPR/Cas9–based gene editing. In brief, the sgRNA target sequences for *TaHsfA1-A/B/D* gene editing were designed using the web-based tool E-CRISPR Design (http://www.e-crisp.org/E-CRISP/). The sgRNA sequences were introduced into the *pBUE411* vector (Xing et al. 2014) via T4 DNA ligase (M0202, New England Biolabs). The resulting constructs were transferred into *A. tumefaciens* strain EHA105 and transformed into wheat cultivar Fielder by *A. tumefaciens*–mediated transformation (Kumar et al. 2019). The transgenic *TaHsfA1-OE* plants and the *Tahsfa1* mutants were validated by PCR and sequencing. The primers used in this study are listed in Supplemental Data Set 6.

Total RNA extraction and RT-qPCR

The first leaves of 7-d-old seedlings were collected for RNA extraction. Total RNA was extracted using TRIzol Reagent (15596018, Thermo Fisher Scientific). The reverse transcription of cDNAs was performed using HiScript II Q RT SuperMix (R223, Vazyme Biotech) according to the manufacturer's recommendations. AceQ qPCR SYBR Green Master Mix (Q121, Vazyme Biotech) was used for RT-qPCR analysis. All primers are shown in Supplemental Data Set 6, and *β-actin* was used as an internal control.

RNA-seq analysis

Samples heat treated for 0, 10, and 30 min were collected for RNA extraction. For each sample, 3 seedlings were randomly sampled as a replicate, and a total of 3 replicates were carried out. RNA-seq libraries were constructed and sequenced on an Illumina NovaSeq 6000 platform to generate 150-bp paired-end reads. The clean reads were trimmed and aligned to the CS reference genome IWGSC RefSeq V1.1 (International Wheat Genome Sequencing Consortium (IWGSC) 2018) using STAR (Dobin et al. 2013). DEGs were identified using the R package DESeq2 according to $\log_2$(fold change) ≥ 1 and $P < 0.05$ (Love et al. 2014). The website Tirticeae-Gene Tribe (TGT, http://wheat.cau.edu.cn/TGT/) was used to perform GO enrichment analysis (Chen et al. 2020). The heatmap of DEGs and the bubble charts of GO enrichment analysis were generated via the R package ggplot2 (Ito and Murphy 2013).

Transcriptional activity assays

For the transcriptional activity assay in yeast (*Saccharomyces cerevisiae*) cells, the CDS of *TaHsfA1* and its truncated fragment were cloned into the *Eco*RI-digested *pGBKT7* (BD) vector (PT3024-1, Clontech Laboratories, Inc.) and transferred into yeast strain Y2HGold. The transformed yeast cells were grown on synthetic dextrose (SD) minimal medium lacking Trp (SD-W) at 30 °C for 2 d and transferred to SD medium lacking Trp and His (SD-W/H) for transcriptional activity assays. For the transcriptional activity assay in *N. benthamiana* leaf epidermal cells, the 2-kb promoter sequences of *TaHsfA2c-A* and *TaHsfA2c-D* were cloned into the *pGWB35* vector (Nakagawa et al. 2007) and separately coexpressed with *pCAMBIA1300-GFP* empty vector or its derivatives including *pCAMBIA1300-TaHsfA1-GFP*, $pCAMBIA1300\text{-}TaHsfA1_{K175R}\text{-}GFP$, or $pCAMBIA1300\text{-}TaHsfA1_{K459R}\text{-}GFP$ in *N. benthamiana*

leaves. These *pCAMBIA1300* derivatives were constructed by inserting the indicated gene sequences into the *Xba*I-digested *pCAMBIA1300-GFP* vector (Baltes et al. 2014). The LUC signal was captured and quantified via a NightSHADE LB 985 plant imaging system.

For the transient transcriptional activation activity assay in wheat protoplasts, the 2-kb promoter sequence of *TaHsfA2c-A* was cloned into the *Hin*dIII/*Kpn*I-digested *pGreenII0800-LUC/35S$_{pro}$-REN* (firefly and Renilla dual reporter) to generate *TaHsfA2c-A$_{pro}$-LUC/35S$_{pro}$-REN* as a reporter (Meng et al. 2013). Wheat protoplasts were isolated from 10-d-old Fielder leaves as described previously (Yoo et al. 2007). In detail, wheat leaves were digested with enzyme solution (1.5% cellulase R10, 0.75% macerozyme R10, 0.6 M mannitol, 10 mM MES, 10 mM $CaCl_2$, and 0.1% BSA, pH 5.7). The obtained protoplasts were washed with W5 solution (154 mM NaCl, 125 mM $CaCl_2$, 5 mM KCl, and 2 mM MES, pH 5.7) and suspended in MMG solution (0.4 M mannitol, 15 mM $MgCl_2$, and 4 mM MES, pH 5.7). Next, 5 μg of the indicated recombinant plasmids coupled with 5 μg of the *TaHsfA2c-A$_{pro}$-LUC/35S$_{pro}$-REN* reporter plasmid was transfected into the protoplasts, followed by incubation in W5 solution for 14 h. The firefly and Renilla LUC activities were determined using a Dual Luciferase Reporter Assay Kit (DL101-01, Vazyme Biotech) on a Spark multimode microplate reader (Tecan Trading AG).

Y2H assay

The CDS of the truncated TaHsfA1 (1-464 amino acids) without autoactivation activity was amplified and cloned into the *pGBKT7* vector (PT3024-1, Clontech Laboratories, Inc.), which was used as a bait to screen a yeast cDNA library derived from Fielder wheat seedlings to identify the candidate TaHsfA1-interacting proteins. Y2H screening was performed according to the user's manual (PT3024-1, Clontech Laboratories, Inc.)

Split-LCI assay

The CDSs of the indicated genes were separately cloned into the K*pn*I/*Sal*I-digested *pCAMBIA1300-nLUC* (nLUC) and *Kpn*I–*Bam*HI-digested *pCAMBIA1300-cLUC* (cLUC) vectors (Chen et al. 2008). The resulting constructs were transformed into *A. tumefaciens* strain GV3101 and coinfiltrated into *N. benthamiana* leaves. Approximately 36 h after infiltration, the LUC signal within the infiltration region was analyzed using the NightSHADE LB 985 plant imaging system (Berthold Technologies). For each assay, 5 independent leaf samples were collected for statistical analysis.

Immunoprecipitation and Co-IP assays

Total proteins were extracted from wheat seedlings using SDS loading buffer (200 mM Tris [pH 6.8], 40% glycerol, 8% SDS, and 20% β-mercaptoethanol) at 100 °C for 5 min. The proteins were separated by SDS–PAGE and transferred to PVDF membranes. The membranes carrying proteins were blocked with 5% milk in TBST containing 0.1% Tween 20 at room temperature for 1 h and incubated with the corresponding antibodies, including anti-SUMO1 antibody (ab5316, Abcam), anti-β-actin antibody (CW0096, CoWin Biotech Corp), anti-GFP antibody (ab32146, Abcam), anti-rabbit IgG-HRP, and antimouse IgG-HRP (Sigma-Aldrich). The proteins were detected using Immobilon Western chemiluminescent HRP substrate (WBKLS, Millipore) under a fluorescence chemiluminescence imaging system (ChemiScope 6100).

For the Co-IP assay in wheat seedlings, total proteins were extracted from 7-d-old Fielder and TaHsfA1-OE seedlings with lysis buffer (50 mM Tris [pH 7.5], 150 mM NaCl, 5 mM EDTA [pH 8.0], 0.1% Triton X-100, and 0.2% NP-40 supplemented with 0.6 mM PMSF, 20 μM MG132, and 1× complete protease inhibitor cocktail) and subjected to TaHsfA1-Flag protein immunoprecipitation using Anti-FLAG M2 Magnetic Beads (M8823, Millipore). The immunoprecipitated proteins were then detected using either anti-Flag antibody (F1804, Sigma-Aldrich) or anti-SUMO1 antibody. For the Co-IP assay in *N. benthamiana* leaf tissues, the full-length CDSs of *TaHsfA1* and *TaHAG1* were cloned into the *Xba*I–*Sal*I-digested *pCAMBIA1300-221-Flag* and *pCAMBIA1300-GFP* vectors, respectively. The *pCAMBIA1300-221-Flag* vector was reconstructed based on the *pBI221* vector (Ying et al. 2010). The fusion plasmids *pCAMBIA1300-TaHsfA1-Flag* or *pCAMBIA1300-221-Flag* and *pCAMBIA1300-TaHAG1-GFP* were coexpressed in *N. benthamiana* leaves. Approximately 36 h after infiltration, total proteins were extracted from infiltrated *N. benthamiana* leaves with lysis buffer as described above. Anti-FLAG M2 Magnetic Beads (M8823, Millipore) were used for TaHsfA1-Flag protein immunoprecipitation. The immunoprecipitated proteins were detected using anti-Flag and anti-GFP antibodies.

SUMOylation assay

The SUMOylation assay was performed as described previously with some modifications (Okada et al. 2009). Briefly, the CDSs of *TaHsfA1*, *TaHsfA1$_{K77R}$*, *TaHsfA1$_{K98R\&K103R}$*, *TaHsfA1$_{K175R}$*, and *TaHsfA1$_{K459R}$* were cloned into the *Eco*RI/*Xba*I-digested *pMAL-c2x* vector (Walker et al. 2010), to generate the *MBP-TaHsfA1*, *MBP-TaHsfA1$_{K77R}$*, *MBP-TaHsfA1$_{K98R\&K103R}$*, *MBP-TaHsfA1$_{K175R}$*, and *MBP-TaHsfA1$_{K459R}$* constructs, respectively. *E. coli* BL21 (DE3) cells were transformed with either *MBP-TaHsfA1*, *MBP-TaHsfA1$_{K77R}$*, *MBP-TaHsfA1$_{K98R\&K103R}$*, *MBP-TaHsfA1$_{K175R}$*, or *MBP-TaHsfA1$_{K459R}$* combined with *pCDFDuet-SUMO1-SCE1a* and *pACYCDuet-SAE1a-SAE2*. The transformed *E. coli* cells were induced at 16, 45, 50, or 55 °C until the OD_{600} reached 1.5, followed by SUMOylation analysis via immunoblotting (anti-MBP antibody, AE016, ABclonal; anti-His antibody, HT501-01, TransGen Biotech; anti-S antibody, 69047-3, Millipore). For the SUMOylation assay during continuous HS treatment, the transformed *E. coli* cells were induced at 50 °C, and 1 mL of cells was collected at the indicated time points for protein level quantification. For NEM treatment, a final concentration of 20 μM NEM was added to the cells

before they were induced, and 1 mL of cells was collected at the indicated time points for subsequent detection. Finally, the SUMOylation level of TaHsfA1 was detected via immunoblotting. The intensities of the TaHsfA1 SUMOylation bands were measured using ImageJ software (http://imagej.nih.gov/ij/). Coomassie brilliant blue staining shows the equal loading of total proteins.

Site-directed mutagenesis

SUMOylation site mutations in TaHsfA1 (K77R, K98R, K103R, K175R, and K459R) were generated by one-step site-directed mutagenesis as previously described (Zheng et al. 2004). In brief, the WT CDS of *TaHsfA1* (the D subgenome copy) was cloned into the *pEASY-Blunt* (CB111-01, TransGen Biotech) vector. The resulting *Blunt-TaHsfA1* vector was used as a template for further PCR amplification. A 50 μL PCR mixture was prepared containing 100 ng *Blunt-TaHsfA1*, 0.6 μM primer pairs harboring certain mutagenized sites (Supplemental Data Set 6), and 25 μL 2 × Phanta Max Master Mix (P515-01, Vazyme). PCR amplification was carried out by preheating the mixture to 94 °C for 3 min, followed by 16 cycles of 94 °C for 1 min, 55 °C for 1 min, and 72 °C for 8 min. The PCR ended with a final incubation step at 72 °C for 1 h. The resulting PCR products were evaluated by agarose gel electrophoresis and treated with the restriction enzyme *Dpn*I (R0176L, New England Biolabs) for 1 h. Approximately 8 μL of the above PCR product was transformed into *E. coli* chemocompetent cells (DH5α) for sequencing analysis and plasmid isolation.

EMSA

The empty vector *pET32a* (69015-3, Novagen) and the expression vector *pET32a-TaHsfA1* (the CDS of *TaHsfA1* was inserted into the *Eco*RI/*Sal*I-digested *pET32a* vector) were separately expressed in *E. coli* BL21 (DE3) cells, and the His tag itself and the His-tagged TaHsfA1, respectively, were induced as previously described (Tian et al. 2022). Oligonucleotide probes were synthesized, and their 5′ ends were labeled with biotin. EMSAs were performed using a Light Shift Chemiluminescent EMSA Kit (20148; Thermo Fisher Scientific) following the manufacturer's instructions. His-TaHsfA1 or His proteins were added to the reaction mixture (1× binding buffer, 50 ng poly(dI·dC), 2.5% [*v*/*v*] glycerol, 0.05% NP-40, 50 mM KCl, 5 mM $MgCl_2$, 2 mM EDTA [pH 8.0], and 1 nM biotin-labeled), followed by incubation at 25 °C for 20 min. The reaction products were loaded onto a 6% native polyacrylamide gel for the detection of biotin-labeled DNAs. The sequences of the biotin probes are listed in Supplemental Data Set 6.

Phylogenetic analysis

To perform phylogenetic analysis, the amino acid sequences of HsfA1 from different plant species were downloaded from Ensembl Plants (http://plants.ensembl.org/index.html). Mega X (Kumar et al. 2018) was employed to construct the phylogenetic tree with the following programs: first, all protein sequences were aligned in Clustal W with default parameters; second, the maximum likelihood (ML) method was used to build a phylogenetic tree with the Poisson model and 1,000 bootstrap replicates; third, the phylogenetic tree was colored, displayed, and annotated on the Interactive Tree of Life website (Letunic and Bork 2021). The alignment and machine-readable tree files are provided as Supplemental Files 1 and 2.

Statistical analysis

In total, at least 3 independent biological replicates (independent sampling events under the same treatment conditions) were employed in each experiment. The numbers of samples (*n*) used for statistical analysis are listed in the figures or figure legends. Error bars represent the SD of each set of data. Asterisks indicate significant differences. Student's *t* test and 1-way ANOVA in GraphPad Prism version 9.0.0 for Windows (GraphPad Software, San Diego, CA, USA) were used for statistical analysis. Statistical data are provided in Supplemental Data Set 7.

Accession numbers

Sequence data from this article can be found in the EMBL library (http://plants.ensembl.org/index.html) under the following accession numbers: *TaHsfA1-A* (TraesCS4A02G322300), *TaHsfA1-B* (TraesCS5B02G556200), *TaHsfA1-D* (TraesCS5D02G553300), *TaHsfA2c-A* (TraesCS1A02G375600), *TaHsfA2c-D* (TraesCS1D02G382900), *TaSUMO1* (TraesCS3D02G419200), TaHAG1 (TraesCS1D02G134200), *TaSIZ1* (TraesCS1A02G065700), *TaMed18* (TraesCS6B02G195600), *TaMed25* (TraesCS5D02G184100), *AtHsfA1a* (AT4G17750), *AtHsfA1b* (AT5G16820), *AtHsfA1d* (AT1G32330), *AtHsfA1e* (AT3G02990), *AtSUMO1* (AT4G26840), *AtSAE1a* (AT4G24940), *AtSAE2* (AT2G21470), *AtSCE1a* (AT3G57870), and *SlHsfA1* (Solyc08g005170). Files of raw sequence reads generated in this study were deposited in the Sequence Read Archive (SRA) under accession number PRJNA890758.

Acknowledgments

We thank Dr. Katsunori Tanaka (Kwansei Gakuin University) for providing the *E. coli* SUMOylation system.

Author contributions

Jie.L. conceived and supervised this project. H.W., M.F., and Y.J. generated wheat materials and performed most of the experiments. H.W., Jie.L., C.D., D.D., Jin.L., X.L., S.L., M.X., Y.Y., Z.N., Q.S., and H.P. interpreted the experimental data. Z.Z., W.W., Y.C., and W.G. analyzed the transcriptome sequencing data. H.W. and Jie.L. wrote the manuscript. Q.S. critically edited the manuscript.

Supplemental data

The following materials are available in the online version of this article.

Supplemental Figure S1. Sequence alignment of HsfA1 proteins derived from Arabidopsis, tomato, and wheat (TaHsfA1-D from the D subgenome).

Supplemental Figure S2. The annotated functional domains or motifs in HsfA1 proteins from Arabidopsis, tomato, and wheat.

Supplemental Figure S3. Thermotolerance of *Tahsfa1* and WT Fielder plants.

Supplemental Figure S4. Loss of *TaHsfA1* largely attenuates the activation of HSP-encoding genes during HS.

Supplemental Figure S5. GO enrichment analysis of DEGs in response to HS in Fielder and *Tahsfa1* lines.

Supplemental Figure S6. GO enrichment of the Fielder-specific and *Tathsfa1*-specific DEGs in response to HS.

Supplemental Figure S7. RT-qPCR validation of the transcriptional changes in HS-responsive genes involved in abiotic stress responses or ROS scavenging and apoptosis.

Supplemental Figure S8. RT-qPCR validation of the HS-triggered transcriptional changes in genes related to plant hormone signaling and translation events or the cell cycle.

Supplemental Figure S9. Sequence alignment of SUMO1 and HsfA1 proteins derived from different plant species.

Supplemental Figure S10. TaHsfA1 interacts with the E3 SUMO ligase TaSIZ1.

Supplemental Figure S11. SUMOylation profiling of wheat total proteins at different time points during HS treatment.

Supplemental Figure S12. Lys459 is a key SUMOylation site in TaHsfA1.

Supplemental Figure S13. Nucleotide sequences of the *TaHsfA2c-A* and *TaHsfA2c-D* promoters.

Supplemental Figure S14. TaHAG1 interacts with TaSUMO1.

Supplemental Figure S15. TaHsfA1 interacts with the Mediator subunits TaMed18 and TaMed25.

Supplemental Data Set 1. List of genes analyzed in this study.

Supplemental Data Set 2. DEGs under heat treatment between *Tahsfa1* and Fielder seedlings.

Supplemental Data Set 3. Differentially expressed *TaHSPs* identified in *Tahsfa1* seedlings compared to Fielder seedlings under heat treatment.

Supplemental Data Set 4. GO enrichment analysis of DEGs in Fielder and *Tahsfa1* seedlings under heat treatment.

Supplemental Data Set 5. TaHsfA1-interacting candidate proteins identified by Y2H screening.

Supplemental Data Set 6. Primers and sequences used in this study.

Supplemental Data Set 7. Statistical analyses of the data obtained in this study.

Supplemental File 1. Multiple sequence alignment of HsfA1s from different plant species.

Supplemental File 2. Newick file of the phylogenetic tree shown in Fig. 1B.

Funding

This work was supported by grants from the National Natural Science Foundation of China (31991214 and 32072055), the Frontiers Science Center for Molecular Design Breeding (MOE), and the 2115 Talent Development Program of China Agricultural University.

Conflict of interest statement. The authors declare no competing interests.

References

Andrási N, Pettkó-Szandtner A, Szabados L. Diversity of plant heat shock factors: regulation, interactions, and functions. J Exp Bot. 2021:**72**(5):1558–1575. https://doi.org/10.1093/jxb/eraa576

Augustine RC, Vierstra RD. SUMOylation: re-wiring the plant nucleus during stress and development. Curr Opin Plant Biol. 2018:**45**(Pt A): 143–154. https://doi.org/10.1016/j.pbi.2018.06.006

Baltes NJ, Gil-Humanes J, Cermak T, Atkins PA, Voytas DF. DNA replicons for plant genome engineering. Plant Cell 2014:**26**(1):151–163. https://doi.org/10.1105/tpc.113.119792

Castro PH, Bachmair A, Bejarano ER, Coupland G, Lois LM, Sadanandom A, van den Burg HA, Vierstra RD, Azevedo H. Revised nomenclature and functional overview of the *ULP* gene family of plant deSUMOylating proteases. J Exp Bot. 2018:**69**(19): 4505–4509. https://doi.org/10.1093/jxb/ery301

Chen Q, Zhang J, Li G. Dynamic epigenetic modifications in plant sugar signal transduction. Trends Plant Sci. 2022:**27**(4):379–390. https://doi.org/10.1016/j.tplants.2021.10.009

Chen H, Zou Y, Shang Y, Lin H, Wang Y, Cai R, Tang X, Zhou J-M. Firefly luciferase complementation imaging assay for protein-protein interactions in plants. Plant Physiol. 2008:**146**(2):368–376. https://doi.org/10.1104/pp.107.111740

Chen Y, Song W, Xie X, Wang Z, Guan P, Peng H, Jiao Y, Ni Z, Sun Q, Guo W. A collinearity-incorporating homology inference strategy for connecting emerging assemblies in the *Triticeae* tribe as a pilot practice in the plant pangenomic era. Mol Plant. 2020:**13**(12):1694–1708. https://doi.org/10.1016/j.molp.2020.09.019

Cohen-Peer R, Schuster S, Meiri D, Breiman A, Avni A. Sumoylation of *Arabidopsis* heat shock factor A2 (HsfA2) modifies its activity during acquired thermotolerance. Plant Mol Biol. 2010:**74**(1–2):33–45. https://doi.org/10.1007/s11103-010-9652-1

Dobin A, Davis CA, Schlesinger F, Drenkow J, Zaleski C, Jha S, Batut P, Chaisson M, Gingeras TR. STAR: ultrafast universal RNA-seq aligner. Bioinformatics 2013:**29**(1):15–21. https://doi.org/10.1093/bioinformatics/bts635

Dong J, LeBlanc C, Poulet A, Mermaz B, Villarino G, Webb KM, Joly V, Mendez J, Voigt P, Jacob Y. H3.1K27me1 maintains transcriptional silencing and genome stability by preventing GCN5-mediated histone acetylation. Plant Cell 2021:**33**(4):961–979. https://doi.org/10.1093/plcell/koaa027

Döring P, Treuter E, Kistner C, Lyck R, Chen A, Nover L. The role of AHA motifs in the activator function of tomato heat stress transcription factors HsfA1 and HsfA2. Plant Cell 2000:**12**(2):265–278. https://doi.org/10.1105/tpc.12.2.265

Duan S, Liu B, Zhang Y, Li G, Guo X. Genome-wide identification and abiotic stress-responsive pattern of heat shock transcription factor family in *Triticum aestivum* L. BMC Genom. 2019:**20**(1):257–257. https://doi.org/10.1186/s12864-019-5617-1

Goodson ML, Hong Y, Rogers R, Matunis MJ, Park-Sarge O-K, Sarge KD. SUMO-1 modification regulates the DNA binding activity of heat shock transcription factor 2, a promyelocytic leukemia nuclear

body associated transcription factor. J Biol Chem. 2001:**276**(21): 18513–18518. https://doi.org/10.1074/jbc.M008066200

Hahn A, Bublak D, Schleiff E, Scharf K-D. Crosstalk between Hsp90 and Hsp70 chaperones and heat stress transcription factors in tomato. Plant Cell 2011:**23**(2):741–755. https://doi.org/10.1105/tpc.110.076018

Hietakangas V, Ahlskog JK, Jakobsson AM, Hellesuo M, Sahlberg NM, Holmberg CI, Mikhailov A, Palvimo JJ, Pirkkala L, Sistonen L. Phosphorylation of serine 303 is a prerequisite for the stress-inducible SUMO modification of heat shock factor 1. Mol Cell Biol. 2003:**23**(8):2953–2968. https://doi.org/10.1128/MCB.23.8.2953-2968.2003

Hsu S-F, Lai H-C, Jinn T-L. Cytosol-localized heat shock factor-binding protein, AtHSBP, functions as a negative regulator of heat shock response by translocation to the nucleus and is required for seed development in *Arabidopsis*. Plant Physiol. 2010:**153**(2):773–784. https://doi.org/10.1104/pp.109.151225

Hu Z, Song N, Zheng M, Liu X, Liu Z, Xing J, Ma J, Guo W, Yao Y, Peng H, et al. Histone acetyltransferase GCN5 is essential for heat stress-responsive gene activation and thermotolerance in *Arabidopsis*. Plant J. 2015:**84**(6):1178–1191. https://doi.org/10.1111/tpj.13076

International Wheat Genome Sequencing Consortium (IWGSC). Shifting the limits in wheat research and breeding using a fully annotated reference genome. Science 2018:**361**(6403):eaar7191. https://doi.org/10.1126/science.aar7191

Ito K, Murphy D. Application of ggplot2 to pharmacometric graphics. CPT Pharmacometrics Syst Pharmacol. 2013:**2**(10):e79. https://doi.org/10.1038/psp.2013.56

Jenuwein T, Allis CD. Translating the histone code. Science 2001:**293**(5532):1074–1080. https://doi.org/10.1126/science.1063127

Kmiecik SW, Drzewicka K, Melchior F, Mayer MP. Heat shock transcription factor 1 is SUMOylated in the activated trimeric state. J Biol Chem. 2021:**296**:100324. https://doi.org/10.1016/j.jbc.2021.100324

Kong X, Luo X, Qu G-P, Liu P, Jin JB. *Arabidopsis* SUMO protease ASP1 positively regulates flowering time partially through regulating FLC stability. J Integr Plant Biol. 2017:**59**(1):15–29. https://doi.org/10.1111/jipb.12509

Kotak S, Port M, Ganguli A, Bicker F, Von Koskull-Döring P. Characterization of C-terminal domains of *Arabidopsis* heat stress transcription factors (Hsfs) and identification of a new signature combination of plant class A Hsfs with AHA and NES motifs essential for activator function and intracellular localization. Plant J. 2004:**39**(1):98–112. https://doi.org/10.1111/j.1365-313X.2004.02111.x

Kumar A, Sharma S, Chunduri V, Kaur A, Kaur S, Malhotra N, Kumar A, Kapoor P, Kumari A, Kaur J, et al. Genome-wide identification and characterization of heat shock protein family reveals role in development and stress conditions in *Triticum aestivum* L. Sci Rep. 2020:**10**(1):7858. https://doi.org/10.1038/s41598-020-64746-2

Kumar R, Mamrutha HM, Kaur A, Venkatesh K, Sharma D, Singh GP. Optimization of *Agrobacterium*-mediated transformation in spring bread wheat using mature and immature embryos. Mol Biol Rep. 2019:**46**(2):1845–1853. https://doi.org/10.1007/s11033-019-04637-6

Kumar S, Stecher G, Li M, Knyaz C, Tamura K. MEGA X: molecular evolutionary genetics analysis across computing platforms. Mol Biol Evol. 2018:**35**(6):1547–1549. https://doi.org/10.1093/molbev/msy096

Kurepa J, Walker JM, Smalle J, Gosink MM, Davis SJ, Durham TL, Sung D-Y, Vierstra RD. The small ubiquitin-like modifier (SUMO) protein modification system in *Arabidopsis*. Accumulation of SUMO1 and -2 conjugates is increased by stress. J Biol Chem. 2003:**278**(9):6862–6872. https://doi.org/10.1074/jbc.M209694200

Letunic I, Bork P. Interactive Tree Of Life (iTOL) v5: an online tool for phylogenetic tree display and annotation. Nucleic Acids Res. 2021:**49**(W1):W293–W296. https://doi.org/10.1093/nar/gkab301

Li B, Gao K, Ren H, Tang W. Molecular mechanisms governing plant responses to high temperatures. J Integr Plant Biol. 2018:**60**(9): 757–779. https://doi.org/10.1111/jipb.12701

Li B, Gao Z, Liu X, Sun D, Tang W. Transcriptional profiling reveals a time-of-day-specific role of REVEILLE 4/8 in regulating the first wave of heat shock-induced gene expression in *Arabidopsis*. Plant Cell 2019:**31**(10):2353–2369. https://doi.org/10.1105/tpc.19.00519

Liebelt F, Jansen NS, Kumar S, Gracheva E, Claessens LA, Verlaan-de Vries M, Willemstein E, Vertegaal ACO. The poly-SUMO2/3 protease SENP6 enables assembly of the constitutive centromere-associated network by group deSUMOylation. Nat Commun. 2019b:**10**(1): 3987–3987. https://doi.org/10.1038/s41467-019-11773-x

Liebelt F, Sebastian RM, Moore CL, Mulder MPC, Ovaa H, Shoulders MD, Vertegaal ACO. SUMOylation and the HSF1-regulated chaperone network converge to promote proteostasis in response to heat shock. Cell Rep. 2019a:**26**(1):236–249.e4. https://doi.org/10.1016/j.celrep.2018.12.027

Lin J, Song N, Liu D, Liu X, Chu W, Li J, Chang S, Liu Z, Chen Y, Yang Q, et al. Histone acetyltransferase TaHAG1 interacts with TaNACL to promote heat stress tolerance in wheat. Plant Biotechnol J. 2022:**20**(9):1645–1647. https://doi.org/10.1111/pbi.13881

Liu H-C, Liao H-T, Charng Y-Y. The role of class A1 heat shock factors (HSFA1s) in response to heat and other stresses in *Arabidopsis*. Plant Cell Environ. 2011:**34**(5):738–751. https://doi.org/10.1111/j.1365-3040.2011.02278.x

Liu H-T, Li B, Shang Z-L, Li X-Z, Mu R-L, Sun D-Y, Zhou R-G. Calmodulin is involved in heat shock signal transduction in wheat. Plant Physiol. 2003:**132**(3):1186–1195. https://doi.org/10.1104/pp.102.018564

Love MI, Huber W, Anders S. Moderated estimation of fold change and dispersion for RNA-seq data with DESeq2. Genome Biol. 2014:**15**(12):550. https://doi.org/10.1186/s13059-014-0550-8

Ma Z, Li M, Zhang H, Zhao B, Liu Z, Duan S, Meng X, Li G, Guo X. Alternative splicing of *TaHsfA2-7* is involved in the improvement of thermotolerance in wheat. Int J Mol Sci. 2023:**24**(2):1014. https://doi.org/10.3390/ijms24021014

Meng Y, Li H, Wang Q, Liu B, Lin C. Blue light-dependent interaction between cryptochrome2 and CIB1 regulates transcription and leaf senescence in soybean. Plant Cell 2013:**25**(11):4405–4420. https://doi.org/10.1105/tpc.113.116590

Miller MJ, Barrett-Wilt GA, Hua Z, Vierstra RD. Proteomic analyses identify a diverse array of nuclear processes affected by small ubiquitin-like modifier conjugation in *Arabidopsis*. Proc Natl Acad Sci U S A. 2010:**107**(38):16512–16517. https://doi.org/10.1073/pnas.1004181107

Miller MJ, Scalf M, Rytz TC, Hubler SL, Smith LM, Vierstra RD. Quantitative proteomics reveals factors regulating RNA biology as dynamic targets of stress-induced SUMOylation in *Arabidopsis*. Mol Cell Proteomics. 2013:**12**(2):449–463. https://doi.org/10.1074/mcp.M112.025056

Mishra SK, Tripp J, Winkelhaus S, Tschiersch B, Theres K, Nover L, Scharf K-D. In the complex family of heat stress transcription factors, HsfA1 has a unique role as master regulator of thermotolerance in tomato. Genes Dev. 2002:**16**(12):1555–1567. https://doi.org/10.1101/gad.228802

Morrell R, Sadanandom A. Dealing with stress: a review of plant SUMO proteases. Front Plant Sci. 2019:**10**:1122. https://doi.org/10.3389/fpls.2019.01122

Nakagawa T, Kurose T, Hino T, Tanaka K, Kawamukai M, Niwa Y, Toyooka K, Matsuoka K, Jinbo T, Kimura T. Development of series of gateway binary vectors, *pGWBs*, for realizing efficient construction of fusion genes for plant transformation. J Biosci Bioeng. 2007:**104**(1): 34–41. https://doi.org/10.1263/jbb.104.34

Nover L, Bharti K, Döring P, Mishra SK, Ganguli A, Scharf KD. *Arabidopsis* and the heat stress transcription factor world: how many heat stress transcription factors do we need? Cell Stress Chaperon. 2001:**6**(3):177–189. https://doi.org/10.1379/1466-1268(2001)006<0177:AATHST>2.0.CO;2

Ohama N, Sato H, Shinozaki K, Yamaguchi-Shinozaki K. Transcriptional regulatory network of plant heat stress response.

Trends Plant Sci. 2017:**22**(1):53–65. https://doi.org/10.1016/j.tplants.2016.08.015

Okada S, Nagabuchi M, Takamura Y, Nakagawa T, Shinmyozu K, Nakayama J-i, Tanaka K. Reconstitution of *Arabidopsis thaliana* SUMO pathways in *E. coli*: functional evaluation of SUMO machinery proteins and mapping of SUMOylation sites by mass spectrometry. Plant Cell Physiol. 2009:**50**(6):1049–1061. https://doi.org/10.1093/pcp/pcp056

Pinto MP, Carvalho AF, Grou CP, Rodríguez-Borges JE, Sá-Miranda C, Azevedo JE. Heat shock induces a massive but differential inactivation of SUMO-specific proteases. Biochim Biophys Acta. 2012:**1823**(10):1958–1966. https://doi.org/10.1016/j.bbamcr.2012.07.010

Qin W, Wang N, Yin Q, Li H, Wu A-M, Qin G. Activation tagging identifies WRKY14 as a repressor of plant thermomorphogenesis in *Arabidopsis*. Mol Plant. 2022:**15**(11):1725–1743. https://doi.org/10.1016/j.molp.2022.09.018

Qu GP, Li H, Lin XL, Kong X, Hu ZL, Jin YH, Liu Y, Song HL, Kim DH, Lin R, et al. Reversible SUMOylation of FHY1 regulates phytochrome a signaling in *Arabidopsis*. Mol Plant. 2020:**13**(6):879–893. https://doi.org/10.1016/j.molp.2020.04.002

Rytz TC, Miller MJ, McLoughlin F, Augustine RC, Marshall RS, Juan Y-T, Charng Y-Y, Scalf M, Smith LM, Vierstra RD. SUMOylome profiling reveals a diverse array of nuclear targets modified by the SUMO ligase SIZ1 during heat stress. Plant Cell 2018:**30**(5):1077–1099. https://doi.org/10.1105/tpc.17.00993

Satyal SH, Chen D, Fox SG, Kramer JM, Morimoto RI. Negative regulation of the heat shock transcriptional response by HSBP1. Genes Dev. 1998:**12**(13):1962–1974. https://doi.org/10.1101/gad.12.13.1962

Scharf K-D, Berberich T, Ebersberger I, Nover L. The plant heat stress transcription factor (Hsf) family: structure, function and evolution. Biochim Biophys Acta. 2012:**1819**(2):104–119. https://doi.org/10.1016/j.bbagrm.2011.10.002

Seo PJ, Park M-J, Lim M-H, Kim S-G, Lee M, Baldwin IT, Park C-M. A self-regulatory circuit of CIRCADIAN CLOCK-ASSOCIATED1 underlies the circadian clock regulation of temperature responses in *Arabidopsis*. Plant Cell 2012:**24**(6):2427–2442. https://doi.org/10.1105/tpc.112.098723

Shi Y, Mosser DD, Morimoto RI. Molecular chaperones as HSF1-specific transcriptional repressors. Genes Dev. 1998:**12**(5):654–666. https://doi.org/10.1101/gad.12.5.654

Sugio A, Dreos R, Aparicio F, Maule AJ. The cytosolic protein response as a subcomponent of the wider heat shock response in *Arabidopsis*. Plant Cell 2009:**21**(2):642–654. https://doi.org/10.1105/tpc.108.062596

Tian X, Qin Z, Zhao Y, Wen J, Lan T, Zhang L, Wang F, Qin D, Yu K, Zhao A, et al. Stress granule-associated TaMBF1c confers thermotolerance through regulating specific mRNA translation in wheat (*Triticum aestivum*). New Phytol. 2022:**233**(4):1719–1731. https://doi.org/10.1111/nph.17865

Walker IH, Hsieh PC, Riggs PD. Mutations in maltose-binding protein that alter affinity and solubility properties. Appl Microbiol Biotechnol. 2010:**88**(1):187–197. https://doi.org/10.1007/s00253-010-2696-y

Wang F, Liu Y, Shi Y, Han D, Wu Y, Ye W, Yang H, Li G, Cui F, Wan S, et al. SUMOylation stabilizes the transcription factor DREB2A to improve plant thermotolerance. Plant Physiol. 2020:**183**(1):41–50. https://doi.org/10.1104/pp.20.00080

Westerheide SD, Anckar J, Stevens SM Jr, Sistonen L, Morimoto RI. Stress-inducible regulation of heat shock factor 1 by the deacetylase SIRT1. Science 2009:**323**(5917):1063–1066. https://doi.org/10.1126/science.1165946

Xing H-L, Dong L, Wang Z-P, Zhang H-Y, Han C-Y, Liu B, Wang X-C, Chen Q-J. A CRISPR/Cas9 toolkit for multiplex genome editing in plants. BMC Plant Biol. 2014:**14**(1):327. https://doi.org/10.1186/s12870-014-0327-y

Xu Y-M, Huang D-Y, Chiu J-F, Lau ATY. Post-translational modification of human heat shock factors and their functions: a recent update by proteomic approach. J Proteome Res. 2012:**11**(5):2625–2634. https://doi.org/10.1021/pr201151a

Xue G-P, Sadat S, Drenth J, McIntyre CL. The heat shock factor family from *Triticum aestivum* in response to heat and other major abiotic stresses and their role in regulation of heat shock protein genes. J Exp Bot. 2014:**65**(2):539–557. https://doi.org/10.1093/jxb/ert399

Ying X-B, Dong L, Zhu H, Duan C-G, Du Q-S, Lv D-Q, Fang Y-Y, Garcia JA, Fang R-X, Guo H-S. RNA-dependent RNA polymerase 1 from *Nicotiana tabacum*. Plant Cell 2010:**22**(4):1358–1372. https://doi.org/10.1105/tpc.109.072058

Yoo CY, Miura K, Jin JB, Lee J, Park HC, Salt DE, Yun D-J, Bressan RA, Hasegawa PM. SIZ1 small ubiquitin-like modifier E3 ligase facilitates basal thermotolerance in *Arabidopsis* independent of salicylic acid. Plant Physiol. 2006:**142**(4):1548–1558. https://doi.org/10.1104/pp.106.088831

Yoo SD, Cho YH, Sheen J. *Arabidopsis* mesophyll protoplasts: a versatile cell system for transient gene expression analysis. Nat Protoc. 2007:**2**(7):1565–1572. https://doi.org/10.1038/nprot.2007.199

Yoshida T, Ohama N, Nakajima J, Kidokoro S, Mizoi J, Nakashima K, Maruyama K, Kim J-M, Seki M, Todaka D, et al. *Arabidopsis* HsfA1 transcription factors function as the main positive regulators in heat shock-responsive gene expression. Mol Genet Genomics. 2011:**286**(5–6):321–332. https://doi.org/10.1007/s00438-011-0647-7

Zadoks JC, Chang TT, Konzak CF. A decimal code for the growth stages of cereals. Weed Res. 1974:**14**(6):415–421. https://doi.org/10.1111/j.1365-3180.1974.tb01084.x

Zhai Q, Li C. The plant mediator complex and its role in jasmonate signaling. J Exp Bot. 2019:**70**(13):3415–3424. https://doi.org/10.1093/jxb/erz233

Zhang H, Zhu J, Gong Z, Zhu J-K. Abiotic stress responses in plants. Nat Rev Genet. 2022:**23**(2):104–119. https://doi.org/10.1038/s41576-021-00413-0

Zhang Z, Li J, Li F, Liu H, Yang W, Chong K, Xu Y. OsMAPK3 phosphorylates OsbHLH002/OsICE1 and inhibits its ubiquitination to activate OsTPP1 and enhances rice chilling tolerance. Dev Cell. 2017:**43**(6):731–743.e5. https://doi.org/10.1016/j.devcel.2017.11.016

Zhao C, Liu B, Piao S, Wang X, Lobell DB, Huang Y, Huang M, Yao Y, Bassu S, Ciais P, et al. Temperature increase reduces global yields of major crops in four independent estimates. Proc Natl Acad Sci USA. 2017:**114**(35):9326–9331. https://doi.org/10.1073/pnas.1701762114

Zhao H, Jan A, Ohama N, Kidokoro S, Soma F, Koizumi S, Mogami J, Todaka D, Mizoi J, Shinozaki K, et al. Cytosolic HSC70s repress heat stress tolerance and enhance seed germination under salt stress conditions. Plant Cell Environ. 2021:**44**(6):1788–1801. https://doi.org/10.1111/pce.14009

Zheng L, Baumann U, Reymond J-L. An efficient one-step site-directed and site-saturation mutagenesis protocol. Nucleic Acids Res. 2004:**32**(14):e115. https://doi.org/10.1093/nar/gnh110

Zheng M, Liu X, Lin J, Liu X, Wang Z, Xin M, Yao Y, Peng H, Zhou D-X, Ni Z, et al. Histone acetyltransferase GCN5 contributes to cell wall integrity and salt stress tolerance by altering the expression of cellulose synthesis genes. Plant J. 2019:**97**:587–602. https://doi.org/10.1111/tpj.14144

Zou J, Guo Y, Guettouche T, Smith DF, Voellmy R. Repression of heat shock transcription factor HSF1 activation by HSP90 (HSP90 complex) that forms a stress-sensitive complex with HSF1. Cell 1998:**94**(4):471–480. https://doi.org/10.1016/S0092-8674(00)81588-3